

SYNTHESIS OF CYCLOPROPYL PEPTIDOMIMETICS  
AS BACE1 INHIBITORS

by

Katrina A. Smith

A Thesis Submitted in Partial Fulfillment  
of the Requirements for the Degree of  
Master of Science in Chemistry

Middle Tennessee State University

2013

Thesis Committee:

Dr. Greg Van Patten, Chair

Dr. Norma K. Dunlap

Dr. D. Andrew Burden

Dr. Andrienne C. Friedli

## ACKNOWLEDGEMENTS

The completion of this thesis wouldn't be possible if it were not for a great many people who enrich and support my life each and every day. Foremost I would like to thank my advisor Dr. Norma Dunlap. Without her overwhelming dedication, wisdom and encouragement, this thesis would not exist. My colleagues and supervisors at the Vanderbilt Center for Neuroscience Drug Discovery allowed for my continuation and completion of bench research using their facilities while still working full-time and for this I am eternally grateful. I want to thank one very special Middle Tennessee State University chemistry professor who, without knowing, has become an inspiration to me as a single mother who made it work (which means: so can I!), Dr. Iriarte-Gross.

Lastly I want to acknowledge how lucky I am to have such truly fantastic, supportive and loving parents. They have seen the highs and lows of this journey and still continue to support my dreams and celebrate my successes. I owe the time I was able to dedicate to the completion of this thesis to my parents who without complaint "spent quality time" with their grand-daughter most nights and days especially leading up to the end. Applause necessary!

## ABSTRACT

Alzheimer's disease (AD) affects over 4.5 million Americans and due to its widespread social and economic impact, development of a drug to slow down or halt progression is imperative. AD is a form of late-life mental deficiency marked by progressive memory and cognitive impairment. Abnormal accumulation of amyloid plaques and neurofibrillary tangles are key biomarkers in AD. Amyloid plaques consist of an insoluble secreted amino acid derivative formed through the proteolytic cleavage of the amyloid precursor protein (APP) by two distinct proteases:  $\beta$ -, and  $\gamma$ -secretase. Much research has been focused on the design and development of a  $\beta$ -secretase (BACE) inhibitor, since animal models have shown repeatedly inhibition of BACE decreases amyloid plaque formation. Peptidomimetics, the mimicking of natural peptide structure, as a means for drug design, was used as an approach to synthesize a series of leucine cyclopropane-derived BACE inhibitors. The synthetic route included nitrocyclopropanation and a transfer hydrogenation as key steps to produce the core structure. Attempts were made to couple the terminal amine of the core to a side chain common to known BACE inhibitors.

## TABLE OF CONTENTS

|  | Page |
|--|------|
| LIST OF FIGURES .....                  | vi   |
| LIST OF TABLES .....                   | viii |
| CHAPTER I: INTRODUCTION .....          | 1    |
| Alzheimer's Disease Pathogenesis ..... | 1    |
| Cholinergic Therapy.....               | 2    |
| AChE Inhibitors .....                  | 3    |
| Tau Pathology.....                     | 3    |
| Amyloid Cascade Hypothesis .....       | 4    |
| Potential Therapeutic Strategies.....  | 7    |
| B-Secretase .....                      | 7    |
| Inhibitors .....                       | 9    |
| Peptidomimetic .....                   | 10   |
| Non-peptidomimetic .....               | 16   |
| Peptidomimetic Design .....            | 19   |
| Cyclopropyl Approach .....             | 19   |
| The Dunlap Laboratory Approach .....   | 25   |
| Nitrocyclopropanation .....            | 26   |
| Objective .....                        | 26   |

## TABLE OF CONTENTS CONT.

|  |    |
|--|----|
| CHAPTER II: MATERIALS AND METHODS .....    | 28 |
| Instruments, Materials, and Reagents ..... | 31 |
| Synthetic Methods .....                    | 32 |
| CHAPTER III: RESULTS AND DISCUSSION .....  | 41 |
| CHAPTER IV: CONCLUSIONS .....              | 47 |
| REFERENCES .....                           | 49 |
| APPENDIX: NMR SPECTROSCOPY DATA .....      | 60 |

## LIST OF FIGURES

|   | Page |
|---|------|
| Figure 1: Hydrolysis of choline by acetylcholinesterase .....   | 2    |
| Figure 2: Acetylcholinesterase (AChE) Inhibitors .....  | 3    |
| Figure 3: APP processing by $\alpha$ -, $\beta$ -, and $\gamma$ -secretase to release A $\beta$ peptide ..... | 5    |
| Figure 4: BACE catalytic activity mechanism .....   | 9    |
| Figure 5: First generation BACE inhibitor – OM99-2 .....  | 11   |
| Figure 6: Statine-based BACE inhibitors .....   | 12   |
| Figure 7: Hydroxyethylene BACE inhibitors .....   | 13   |
| Figure 8: Hydroxyethylamine BACE inhibitors .....   | 14   |
| Figure 9: Macrocyclic BACE inhibitors .....   | 15   |
| Figure 10: Diamino isonicotinamide BACE inhibitor .....   | 16   |
| Figure 11: Non-peptidomimetic BACE inhibitors .....   | 18   |
| Figure 12: Cyclopropyl incorporation strategies .....   | 20   |
| Figure 13: Cyclopropane-derived Renin inhibitors .....  | 21   |
| Figure 14: Intramolecular cyclopropanation using a rhodium catalyst .....                                     | 22   |
| Figure 15: Cyclopropane-derived HIV-1 protease inhibitors .....   | 23   |
| Figure 16: Multi-component condensation cyclopropanation synthesis .....                                      | 23   |
| Figure 17: Simmons-Smith cyclopropanation .....   | 24   |
| Figure 18: Wipf's cyclopropyl peptide isosteres .....   | 24   |
| Figure 19: The Dunlap laboratory cyclopropyl peptidomimetic synthesis .....                                   | 25   |
| Figure 20: Nitrocyclopropanation using bromonitromethane .....  | 26   |
| Figure 21: Synthesis of Cbz-leucine cyclopropyl nitro alcohol .....   | 28   |
| Figure 22: Reduction of the Cbz protecting group .....  | 29   |
| Figure 23: BACE side chain coupling reaction .....  | 30   |
| Figure 24: Benzoic acid coupling reaction .....   | 30   |

|   |    |
|---|----|
| Figure 25: Unstable di-amine synthesis .....                        | 30 |
| Figure 26: Ester series amide synthesis .....                       | 41 |
| Figure 27: Previous nitro reduction attempts on serine series ..... | 42 |
| Figure 28: Transfer hydrogenation desired reaction .....            | 43 |
| Figure 29: Nucleophile attack on cyclopropyl ring .....             | 46 |

## LIST OF TABLES

|  | Page |
|--|------|
| Table 1: Transfer hydrogenation reaction results ..... | 44   |

## CHAPTER I: INTRODUCTION

### **Alzheimer's Disease Pathogenesis.**

According to estimates from the 2000 U.S. Census Bureau, Alzheimer's disease (AD) affects 4.5 million Americans and should increase to 13.2 million by the year 2050.<sup>1</sup> This staggering statistic inspired researchers to work toward the prevention, treatment, and/or cure of this destructive disease. AD is a form of late-life mental deficiency marked by progressive memory and cognitive impairment, unstable behavior such as paranoia, and loss of social appropriateness.<sup>2</sup> Due to its widespread economic and social impact, the United States Congress has signed into law the National Alzheimer's Project Act to create and maintain a national plan to fight AD.<sup>3</sup> The national plan includes a research funding investment of \$156 million over the next two years to propel the development of effective AD treatments.

As an individual ages, amyloid plaques and neurofibrillary tangles can accumulate in the brain. AD patients have plaque and tangle formation in parts of the brain associated with memory and cognitive functioning.<sup>6</sup> The density of the amyloid plaques and neurofibrillary tangles results in neuronal and synaptic loss. The degree of cognitive impairment can be based on the amount of synaptic loss between neurons.<sup>7, 8</sup> There is no known natural defense against neural circuitry loss, thus substantial research has been dedicated to combat degenerative changes in the brain characteristic of AD.<sup>9</sup>

In 1906 Alois Alzheimer was the first to notice the connection of amyloid plaque formation in the cerebral cortex to a series of symptoms such as memory loss and

cognitive dysfunction.<sup>4</sup> Close to eighty years later, Glenner and Wong were the first to purify the plaques and sequence the main component, the amyloid  $\beta$ -protein ( $A\beta$ ).<sup>5</sup> A few years later, several scientists discovered neurofibrillary tangles that consisted of abnormally phosphorylated  $\tau$  (tau) protein.<sup>10-12</sup> These two historic discoveries were the first neurochemical clues to understanding the pathogenesis of AD.

*Cholinergic Therapy.* An early observation of the cause of dementia was the severe deficiency of acetylcholine (ACh) levels in the brain.<sup>2</sup> Choline is used to synthesize ACh, which acts at cholinergic neurons. Cholinergic neurons are located near the nucleus basalis, a part of the brain associated with learning and memory. To maintain an equilibrium between the synthesizing and hydrolyzing enzymes, is to ensure proper brain function.<sup>17</sup> The simplicity of cholinergic pathology led researchers to focus on increasing ACh levels by protecting released ACh from hydrolysis by the serine protease acetylcholinesterase (AChE), shown in Figure 1. It was thought that activating Ach by inhibiting AChE would increase cholinergic activity and improve memory dysfunction.<sup>18</sup>

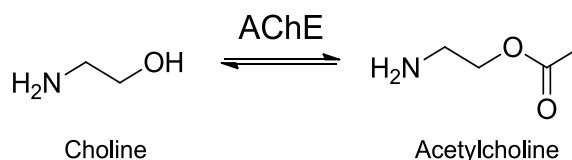


**Figure 1: Hydrolysis of choline by acetylcholinesterase**

*AChE Inhibitors.* The first AChE inhibitor to become available to AD patients was tacrine in 1993.<sup>19</sup> Due to tacrine's long half-life, dosing limitations became problematic and caused a number of harmful side effects. There are three AChE inhibitors on the market today: donepezil, galantamine, and rivastigmine (Figure 2). Donepezil can treat all stages of AD while galantamine and rivastigmine are used for patients with mild to moderate symptoms. Although the simplicity of cholinergic therapy is promising for symptomatic relief, the need to halt the progression of the disease is ever present.<sup>2, 20</sup>

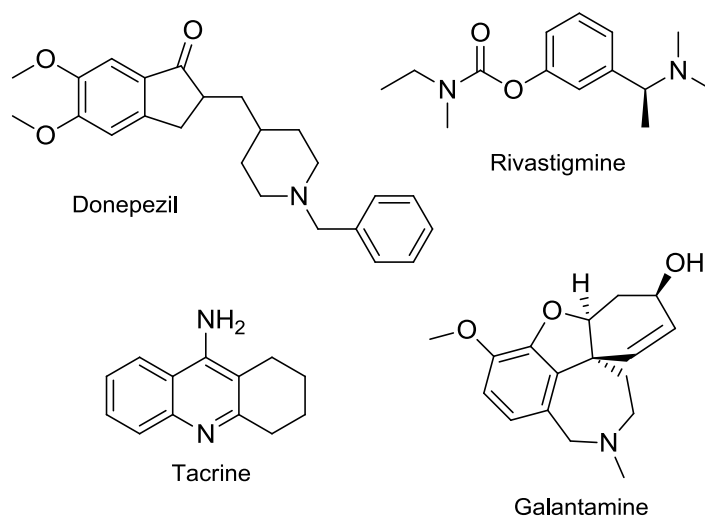


**Figure 2: Acetylcholinesterase (AChE) inhibitors**

*Tau Pathology.* A soluble cytoplasmic protein, tau is responsible for stabilizing microtubules in cytoskeletal organelles.<sup>10</sup> The microtubule system is critical to the

transport of materials between axons.<sup>13</sup> Once tau is phosphorylated, it can accumulate in and around neurons, having a negative effect on microtubule stability.<sup>14</sup> Affecting all areas of the brain, hyperphosphorylated tau structurally forms insoluble paired helical filaments which become the main component of neurofibrillary tangles.<sup>11, 12</sup> Tau degeneration leads to progressive dementia and is a part of the amyloid cascade hypothesis.<sup>7-9, 15, 16</sup>

*Amyloid Cascade Hypothesis.* An amyloid plaque is an A $\beta$  precipitate which can accumulate in the walls of blood vessels and around neurons in areas contributing to memory in the brain.<sup>21-23</sup> The amyloid plaques, with the A $\beta$  core, are surrounded by abnormal synapses and faulty neurons. The exact function and cause of amyloid formation is still unknown.<sup>9</sup>

The protein responsible for A $\beta$  formation is called the amyloid precursor protein (APP); a polypeptide expressed in multiple cells throughout the body.<sup>2</sup> All cells expressing APP generate A $\beta$ , which has the ability to circulate, cross the blood brain barrier, and accumulate around cerebral neurons. APP is processed through the secretory pathway in the cell by a series of proteolytic cleavages completed by three distinct proteases:  $\alpha$ -,  $\beta$ -, and  $\gamma$ -secretase.<sup>2, 9, 15, 24</sup> The secreted derivatives, known as residues, are released into the cerebral spinal fluid and dissolved in the brain. Processing of APP within the A $\beta$  domain is carried out by  $\alpha$ -secretase which releases a large, soluble fragment. Retained is a COOH-terminal fragment which can undergo additional processing by  $\gamma$ -secretase to release a p3 peptide. Alternatively,  $\beta$ -secretase ( $\beta$ -site APP-

cleaving enzyme (BACE)) can produce a slightly smaller residue than  $\alpha$ -secretase, retaining a COOH-terminal fragment which when cleaved by  $\gamma$ -secretase releases the A $\beta$  peptide (Figure 3).<sup>25, 26</sup>

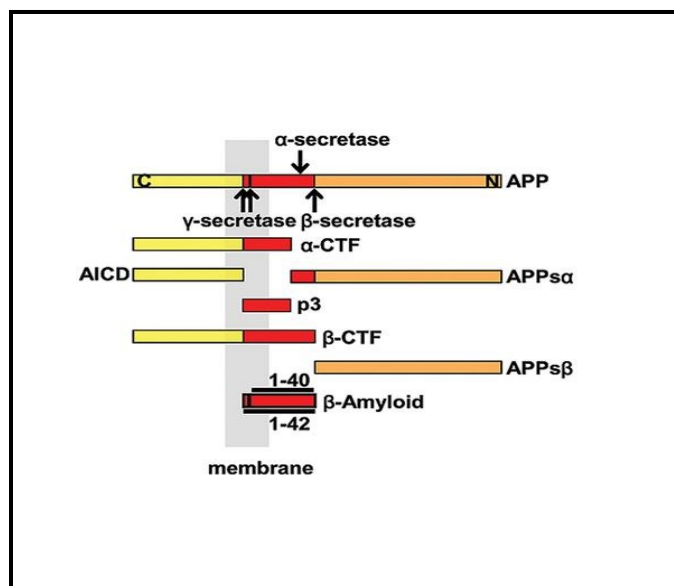


**Figure 3: APP processing by  $\alpha$ -,  $\beta$ -, and  $\gamma$ -secretase to release A $\beta$  peptide.**<sup>124</sup>

The  $\gamma$ -secretase has the ability to release an A $\beta$  peptide 40 (A $\beta$ 40) or 42 (A $\beta$ 42) amino acids in length. A normal metabolic processing of APP will generate a small amount of the abnormal A $\beta$ 42. The ratio between A $\beta$  40 and A $\beta$  42 is tightly regulated; however it is hypothesized regulation declines as part of the natural aging process. Increased production of A $\beta$ 42, since insoluble in cerebral spinal fluid, will lead to aggregation and inevitable plaque formation.<sup>2, 8, 9</sup>

APP gene mutations are the cause of progressive, enhanced buildup of A $\beta$  which initiates a complex cascade of events responsible for neurodegeneration.<sup>8, 15, 16, 27</sup> As A $\beta$

plaques accumulate, synaptic and neuronal injury become apparent,<sup>28</sup> modified kinases hyperphosphorylate tau protein to affect axon transport,<sup>14</sup> and deficiencies in neurotransmitters initiate cell death. This extensive cascade of events leads to dementia and cognitive failure, symptoms characteristic of AD.<sup>8, 9, 15, 16</sup>

APP mutations are gain-of-function mutations by elevating A $\beta$  production.<sup>2</sup> Most mutations support cleavage of APP by BACE, inducing increased production of A $\beta$ 42.<sup>29-</sup><sup>31</sup> Mutations to APP processing occur before abnormal phosphorylation of tau (in AD patients); thus suggesting A $\beta$  toxicity is tau dependent.<sup>32</sup> Several cases exist where severe precipitation of neurofibrillary tangles is present without the presence of amyloid plaques.<sup>33</sup> Establishment of faulty functioning on APP is a main component of AD pathogenesis.<sup>8, 9, 34</sup>

The degree of cognitive impairment and AD progression does not correlate well with amyloid plaque deposition.<sup>15</sup> However the concentration of soluble A $\beta$  residues can be used to determine severity of dementia. The complete understanding of neuronal injury inflicted by insoluble A $\beta$ 42 has yet to be defined *in vivo*.<sup>15</sup> A $\beta$  plaques consist of soluble and insoluble APP protein fragments. The collection of amyloid plaques may serve as basins for soluble A $\beta$  to be dispersed throughout the brain and be responsible for synaptic and neuronal damage.<sup>2</sup> It is difficult to determine whether the soluble or insoluble A $\beta$  peptide is more toxic than the other or if each are equally important in AD pathogenesis.<sup>9</sup>

*Potential Therapeutic Strategies.* Due to widespread acceptance of the amyloid cascade hypothesis, much research is dedicated to treatment options associated with APP processing. Several strategic areas of potential therapeutic options include prevention of neurodegeneration by A $\beta$  build-up, enhancing solubility of A $\beta$  peptides, introducing small molecules to prevent plaque assembly, or production of BACE or  $\gamma$ -secretase inhibitors.<sup>2, 9, 15</sup> The Elan Corporation in the mid 1990s was the first to successfully block  $\gamma$ -secretase activity *in vitro*.<sup>35</sup> Since the Elan Corporation's first  $\gamma$ -secretase inhibitor, several have moved forward to clinical trials within the last ten years.<sup>36-38</sup> The clinical trials have all been unsuccessful at varying stages with all exhibiting harmful side effects. Speculation has risen among researchers whether  $\gamma$ -secretase inhibitors are practical therapeutic strategy for AD.<sup>35</sup> More research is focused on BACE inhibition because it is the first step (rate-limiting) toward toxic plaque accumulation.

*$\beta$ -Secretase.* A critical part of A $\beta$  peptide production, BACE, discovered in 1992, was finally fully characterized in 1999 by five separate research groups concurrently.<sup>39-43</sup> Several groups were able to identify the enzyme using human genome databases, from previous evidence suggesting one of the secretases involved in APP processing was an aspartyl protease.<sup>40, 42, 43</sup> A biochemistry group isolated and purified the active enzyme directly from brain membranes while another group isolated BACE cDNA using its ability to increase A $\beta$  production.<sup>39</sup> The final characterization of BACE led to researchers pursuing this enzyme as a promising pharmacological target to fight AD.

BACE is a type I integral membrane glycoprotein. It has a large extracellular domain of 434 amino acids with only 24 amino acids in the intracellular domain.<sup>44</sup> Another  $\beta$ -secretase enzyme with similar structure and homology but different tissue distribution, localization, and substrate specificity was also identified from human genome databases.<sup>45</sup> Demonstrating cleavage of APP within the A $\beta$  domain, this enzyme named BACE2, was found to not play a role in plaque formation.<sup>46</sup> BACE1 extracellular domain contains the residues needed for catalytic activity (Figure 4).<sup>47</sup> Two highly conserved aspartic acid residues, Asp 32 and 228, are contained within the active-site enabling the enzyme to be an aspartyl protease.<sup>44, 48</sup> Due to the acidic intracellular compartments, BACE optimum pH is 4 – 4.5.<sup>49</sup> The active-site is characterized by hydrophobic and hydrophilic pockets controlled by conformational changes of the “flap.”<sup>47, 50-52</sup> A flexible  $\beta$ -hairpin, the flap regulates access to the active site and sets BACE in the correct geometry for proper enzyme functioning. Two water molecules along with Asp 32 and 228 use acid-base mechanisms to open the flap (in active conformation), cleave peptide bond, and close flap (in inactive conformation).<sup>50, 53</sup>

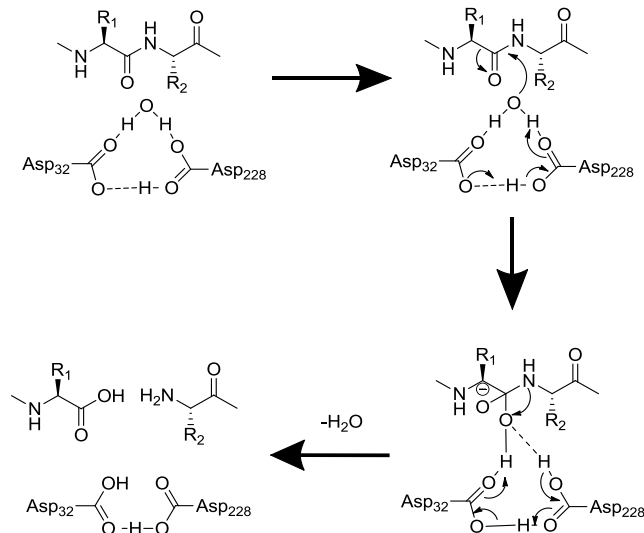


**Figure 4: BACE catalytic activity mechanism**<sup>50, 53</sup>

While the features of the BACE1 enzyme are well known, its function and regulation is not completely understood. Since BACE is located in and around neurons and transported to axons in the cell<sup>54</sup>, it may play a role in myelination since mice devoid of BACE display hypo-myelination.<sup>55</sup> However, this function is independent of A $\beta$  production, as overexpression of BACE in mice causes neurodegeneration.<sup>56</sup> BACE expression in platelets may be an indication of function in the inflammatory response.<sup>57</sup> Much evidence exists confirming an association between inflammation response and AD, yet further research is needed to explain the complex molecular interactions.<sup>58</sup>

*Inhibitors.* Although the function of BACE is unclear, the aim to inhibit BACE activity in the cell is evident. Animal models have shown repeatedly that the inhibition of BACE decreases the amount of A $\beta$  in the brain, therefore reducing harmful plaque formation and the downstream steps in the pathogenesis of AD.<sup>59-61</sup> In a knockout mice

study, all animals without BACE expression did not produce A $\beta$  plaques. Crossing those mice with mice having an overproduction of human APP rescued memory dysfunction, suggesting that an effective treatment for AD could be found.<sup>59-61</sup> In another knockout mice study, mice showed only minor behavioral changes, suggesting that if an effective BACE inhibitor is synthesized, side effects could be minimal.<sup>61, 62</sup> Effective selectivity development over BACE-2 and cathepsin D, the other aspartyl proteases found in human cells, is required. An optimal BACE inhibitor needs to be somewhat water soluble to reach the aqueous, acidic environment of the BACE active site and yet be hydrophobic enough to have the ability to penetrate the blood brain barrier (BBB).<sup>15</sup>

*Peptidomimetic.* The first generation peptidic BACE inhibitor synthesized with high potency was a transition-state analog, OM99-2 (Figure 5).<sup>63</sup> This novel inhibitor was designed with knowledge of BACE substrate specificity and contained a hydroxyethylene transition-state isostere. The eight residue long inhibitor was extremely potent (1.6 nM) due to its distinct positioning of each residue in the peptide chain. With further characterization of an OM99-2 X-ray crystal structure within the BACE active-site, one of the alanine residues formed an unwanted “kink” in the backbone.<sup>52</sup> By replacing the alanine with a valine, OM00-3 was synthesized and generated higher activity than OM99-2 (0.6 nM).<sup>64</sup> Unfortunately, neither of these two inhibitors exhibited the ability to cross the BBB, but were able to give insight into the binding interactions of the active site to advance inhibitor design.

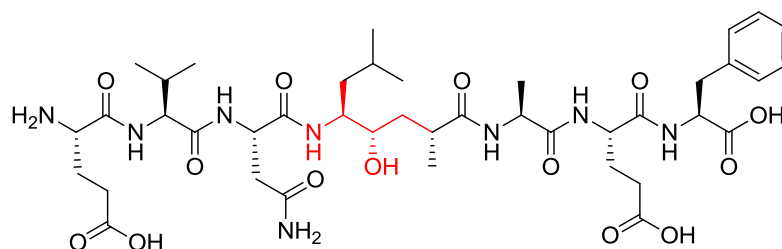


**Figure 5: First generation BACE inhibitor - OM99-2  
(hydroxyethylene isostere)**

In order to maintain biological activity but have the ability to penetrate the BBB, researchers began looking at peptide replacements to lessen the peptidic nature of potential BACE inhibitors. Since the amino acid preference of the BACE active site is quite broad, a variety of side chains can interact well with the active-site.<sup>64, 65</sup> Several inhibitors have been reported with a statine-based central core and an acidic tetrazole ring (Figure 6).<sup>66, 67</sup> These bioisosteric replacements maintained good potency (5.6 – 1.2 nM) and were found to inhibit BACE in cultured cells.

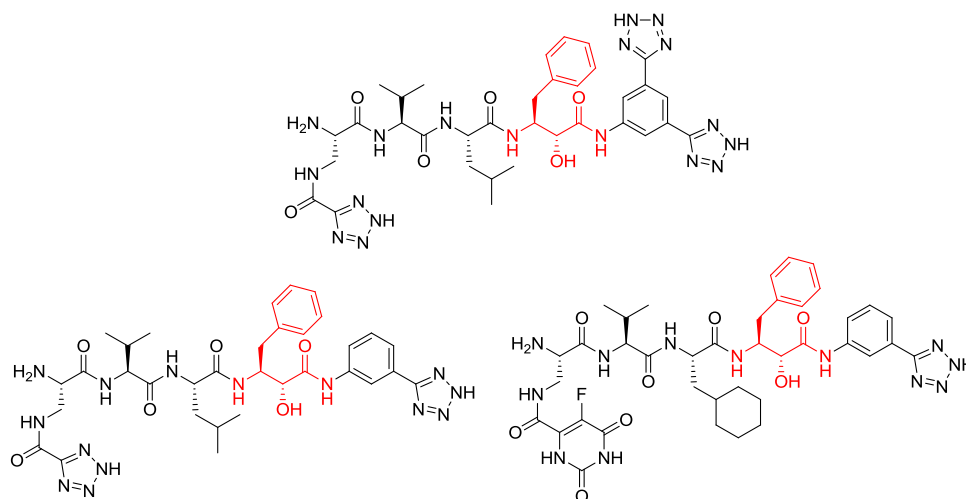


**Figure 6: Statine-based BACE inhibitors  
(phenylnorstatine core)**

To further explore peptide alternatives, multiple hydroxyethylene-based (HE) inhibitors have been synthesized (Figure 7).<sup>68-72</sup> An N-terminal isophthalamide side chain (red in Figure 7), compound **1** proved to improve cell penetration and generate good enzymatic inhibition (30 nM).<sup>69</sup> With the addition of a methoxy group near the core, compound **2** potency increased ten-fold leading to better selectivity against cathepsin D.<sup>71</sup> Moreover, deletion of the amide linkage (blue in Figure 7) in compound **2** to form compound **3**, decreased potency (140 nM) showing the interaction between the amide bond and the active-site is important in generating good activity.<sup>72</sup>

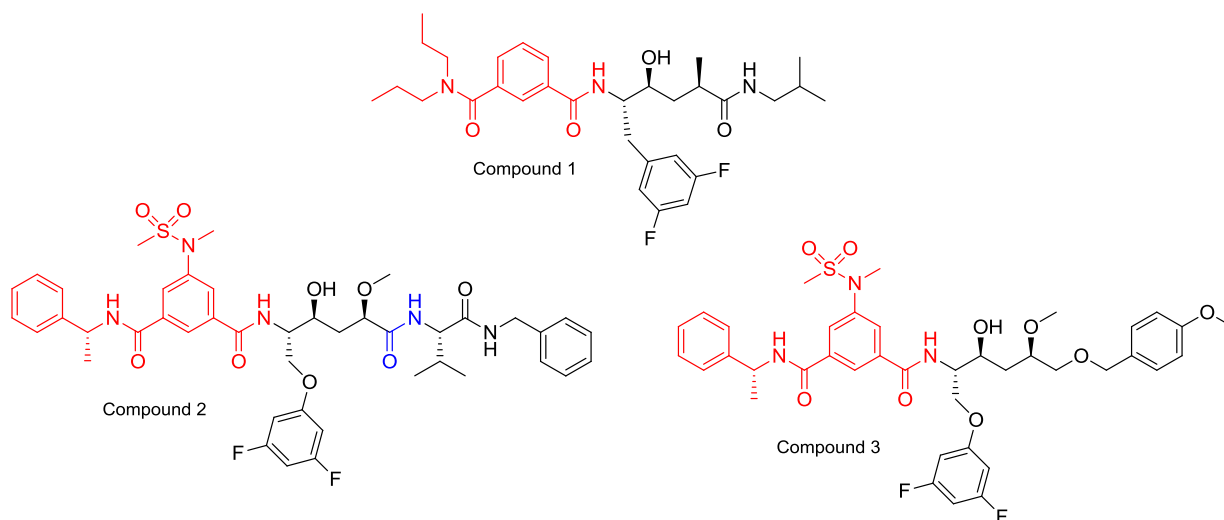


**Figure 7: Hydroxyethylene BACE inhibitors (isophthalamide side chain and amide bond)**

Another series of BACE inhibitors, hydroxyethylamine-based (HEA), has been able to further characterize the drug interaction preferences of the BACE enzyme assuming the basic nitrogen contributes to an increase in potency.<sup>73, 74</sup> HEA cores are made up of a hydroxy group with the *R* configuration (opposite of HE series) and an amine linkage on the C-terminal end of the scaffold (Figure 8). With the isophthalamide side chain functionalized in conjunction with a primary amine, desirable potency was observed for compound **4** along with increased selectivity.<sup>75</sup> As a result of poor metabolic stability, researchers replaced the isophthalamide side chain with an acyclic sulfone (compound **5**).<sup>76</sup> Although increased potency was observed, the compound had greater affinity for cathepsin D. Using the X-ray crystal structure of compound **6** interacting with BACE, analysis shows strong hydrogen bonding between the two catalytic aspartic acids and the hydroxy group as well as the secondary amine.<sup>73</sup> This

BACE inhibitor expressed significant enzymatic inhibition (1 nM), good selectivity and remarkable *in vivo* results.<sup>73, 77, 78</sup>

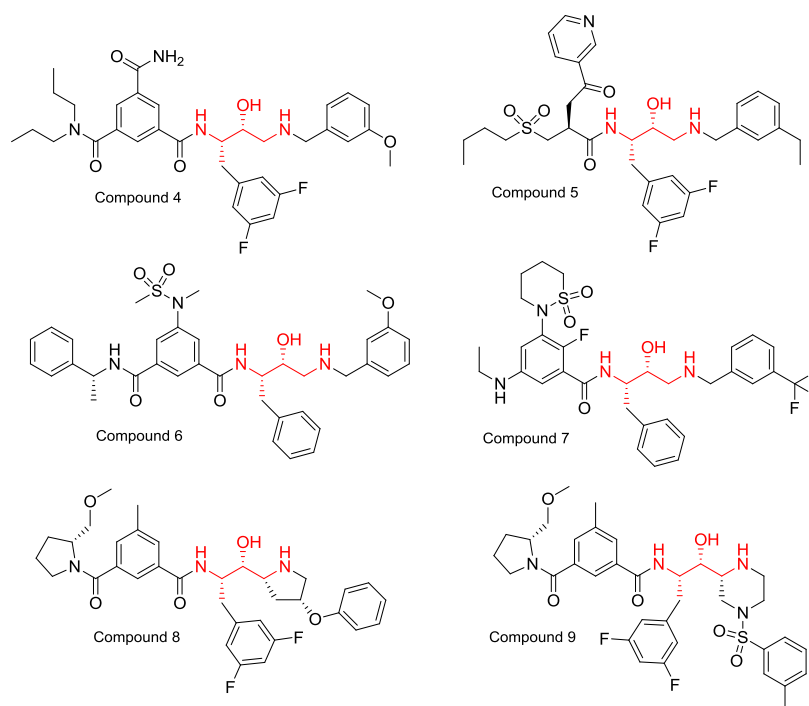


**Figure 8: Hydroxyethylamine BACE inhibitors  
(HEA core)**

The first BACE inhibitor to achieve oral bioavailability came from GlaxoSmithKline in 2007.<sup>79</sup> The hydroxyethylamine isostere core (shown red in Figure 8) of compound 7 achieved good potency (4 nM), excellent selectivity over the other aspartyl proteases, and showed the ability to reduce A $\beta$  levels in the brain of APP transgenic mice. Investigations into conformationally constrained replacements in the

peptide chain, pyrrolidine inhibitors were developed (compounds **8** and **9**).<sup>80, 81</sup> While these restricted BACE inhibitors showed good enzymatic inhibition (low nM range) *in vitro*, they were not selective for BACE and metabolically unstable.

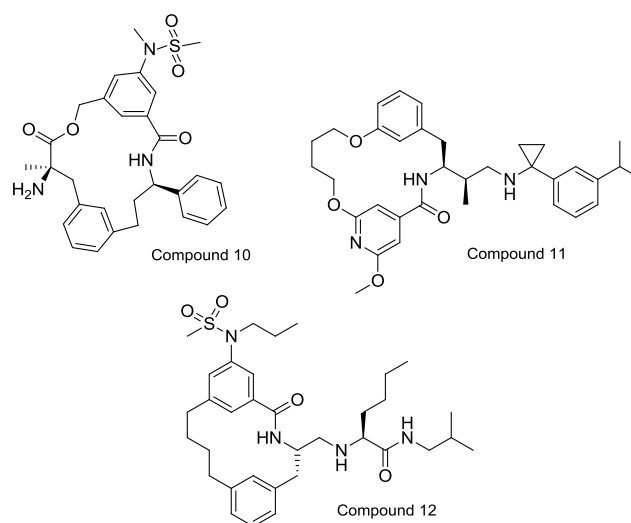


**Figure 9: Macrocyclic BACE inhibitors**

In order to stabilize the active conformation needed to achieve good potency, macrocyclization has been used to pre-organize several compounds by restraining conformational freedom (Figure 9).<sup>82-86</sup> This strategy is possible due to the open nature of the BACE active site subsites.<sup>87</sup> Several examples were found to maintain high potency, seen in other BACE inhibitors, and improve membrane permeability (compounds **10-12**).<sup>84-86</sup> To increase the interaction between inhibitor and the catalytic Asp found in the BACE active-site, researchers introduced a primary amine on the C-

terminal end of the compound with a diamino-isonicotinamide core (Figure 10), which exhibited high potency but low bioavailability.<sup>88, 89</sup> An exploration of different substituents on the phenyl group of compound **13**<sup>88</sup> gave some improvement of enzymatic inhibition *in vitro* but led to no enhancement of pharmacokinetic properties due to poor brain penetration.<sup>90</sup>

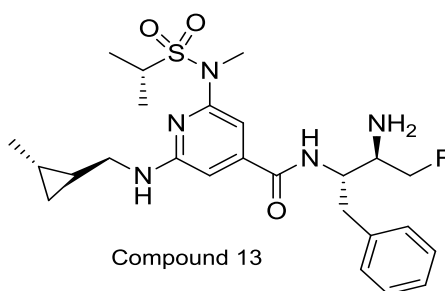


**Figure 10: Diamino isonicotinamide BACE inhibitor**

*Non-peptidomimetic.* Several concerns exist with the use of peptidomimetics as BACE inhibitors; the large active-site and need for proficient brain penetration has lead numerous researchers to devote efforts toward exploring non-peptidomimetic inhibitors of BACE with a new chemical backbone (Figure 11). Using high throughput screening, an acylguanidine-based inhibitor was optimized to achieve compound **14**.<sup>91</sup> Through the X-ray crystal structure of BACE and compound **14** complexed together, analysis of the interactions between the functional groups of the inhibitor and the residues of the active-site were examined. The N-acylguanidine core (shown red in Figure 11) interacts with

the catalytic aspartates and the N-terminal substituents which creates hydrogen bonding between the inhibitor and two amino acids by making use of the water molecules associated with BACE.<sup>91</sup> Acylguanidine-based compounds have poor selectivity and permeability which are major drawbacks to this group of non-peptidomimetic BACE inhibitors.<sup>92-94</sup>

Extending the inhibitor to enhance its interactions with the large active-site, researchers developed a series of aminoquinazoline-based inhibitors (Figure 11). Modifications to the initial hit found in high throughput screening of the Wyeth corporate library developed compound **15**.<sup>95</sup> Analysis of the X-ray structure determined the cyclohexane occupies a distinct subsite and stabilizes BACE in its open conformation, as opposed to peptidomimetic BACE inhibitors. Enhancement of compound **15** to compound **16**, which proved to be an effective inhibitor (11 nM) decreasing A $\beta$  levels up to 70% in rats. As seen with other peptidomimetic and non-peptidomimetic BACE inhibitors, inhibitor **16** has difficulties penetrating the BBB as well as not being selective over the other aspartyl proteases.<sup>95</sup>

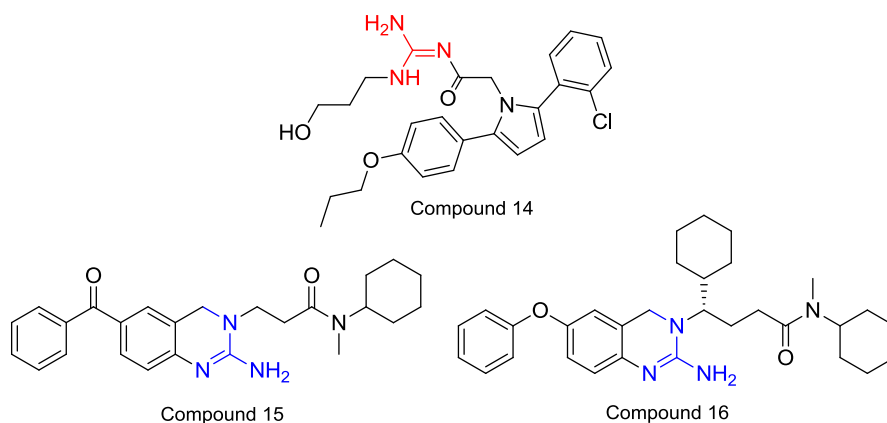


**Figure 11: Non-peptidomimetic BACE inhibitors  
(acylguanidine and aminoquinazoline)**

Based on the amyloid cascade hypothesis, development of a BACE inhibitor drug candidate capable of crossing the BBB, selective over other aspartyl proteases, and with high enzymatic inhibition *in vitro* and *in vivo* is crucial. Recently a BACE inhibitor, CTS-21166 (structure undisclosed), successfully completed Phase I clinical trials.<sup>96</sup> CTS-21166 exhibited good potency (3 nM) and selectivity (around 100-fold better for BACE over cathepsin D).<sup>97</sup> A one-third decrease in A $\beta$  levels of transgenic mice over a six week period, led to the first clinical trial of CTS-21166 in 2008.<sup>98,99</sup> Assessment of safety and initial A $\beta$  reaction to CTS-21166 was conducted on healthy, young males. Results from the first Phase I trial allowed a second Phase I trial to administer the drug orally. Reduction of A $\beta$  levels were seen which is encouraging for the development of a successful BACE inhibitor.<sup>87,100</sup>

## **Peptidomimetic Design.**

Peptidomimetic compounds have a core structure mimicking that of a natural peptide. They conserve the ability to interact with biological targets and have the potential to overcome the issues associated with a normal peptide such as rapid excretion, limited stability, and poor bioavailability.<sup>101</sup> The use of peptides as drug candidates is a common strategy because most peptides can be easily synthesized with large structural diversity. The linker in a peptide chain is the amide bond; this bond is semi-rigid and has partial double bond characteristics.<sup>102</sup> This key feature of peptides is crucial to interactions and cell recognition. Amide bond replacements along with cyclization, amino acid substituents, and N-methylation are all strategies used in the synthesis of peptidomimetic drug design.<sup>102-104</sup> Conformational constraints of the amide bond are employed in peptidomimetic synthesis to orient the amino acid side chains into the most beneficial position to achieve optimum enzymatic inhibition. Isosteric replacements modify the backbone of a peptide improving pharmacological properties.<sup>101</sup>

*Cyclopropyl Approach.* Critical to the development of successful peptidomimetic inhibitors is enhanced pharmacological properties. Manipulation of peptidic structure can be a way to increase the interaction of the peptidomimetic inhibitor with the active site. Several studies have shown that conformationally constraining the structure of a peptidomimetic drug candidate improves selectivity and pharmacokinetic profile.<sup>105</sup> The constraint of the backbone can influence metabolic properties.<sup>106</sup> Researchers have used cyclopropane derivatives as isosteric amide bond replacements in order to increase

metabolic stability and provide a way to position side chains in ideal orientations for optimum binding.<sup>107-112</sup>

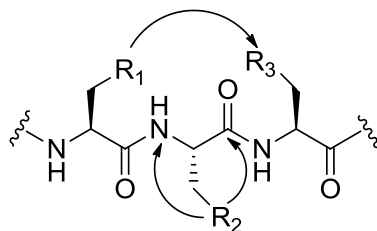


**Figure 12: Cyclopropyl incorporation strategies<sup>111</sup>**

Strategies to incorporate a cyclopropane ring into the peptidomimetic structure include bond formation between two side chains, a side chain to the backbone and insertion into the peptide backbone (Figure 12). Selection of cyclization site or insertion influences conformation and therefore binding effects of the molecule. Cyclopropane-derived structures restrict the movement of the amide bond which can influence pharmacokinetic properties. When amide bond flexibility is greatly reduced, side chains are fixed in beneficial conformations to achieve higher affinity for biological targets.

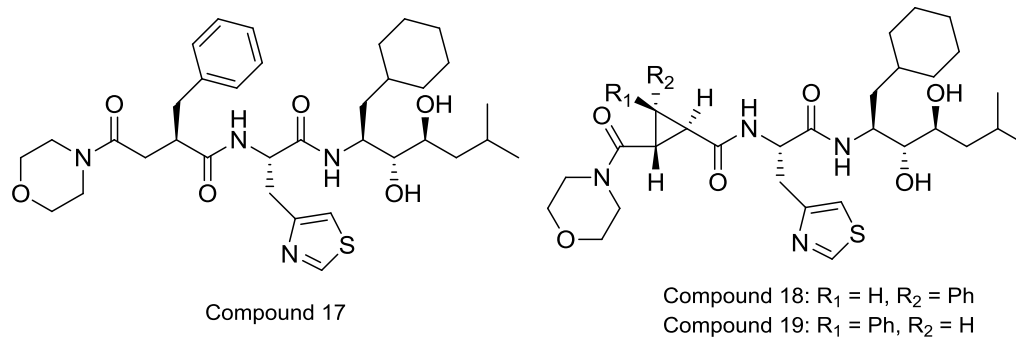


**Figure 13: Cyclopropane-derived Renin inhibitors**

Martin, *et al.* were the first to investigate the use of cyclopropane-derived peptidomimetics in the development of aspartyl protease renin inhibitors.<sup>113</sup> Introduction of the cyclopropane ring was used to orient the phenyl side chain of the potent renin inhibitor compound **17** (Figure 13). Synthesis of the cyclopropane ring involved using a rhodium catalyst to complete an intramolecular cyclopropanation of an alkene with a diazoester (scheme in Figure 14).<sup>111</sup> Through the use of the rhodium catalyst, numerous compounds were made of dihydroxy and hydroxyethylene peptidomimetics.<sup>109, 110</sup> The rigid compound **18** proved to be equipotent to its original counterpart while its enantiomer (compound **19**) lost a considerable amount of potency.<sup>113</sup> While the constrained conformation did not increase enzymatic activity, the results still supported the use of cyclopropane-derivatives as an effective peptidomimetic rigid replacement.<sup>114</sup>

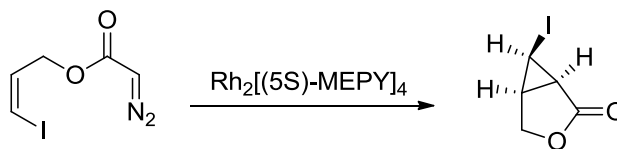
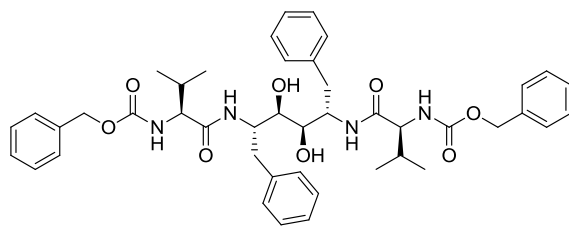
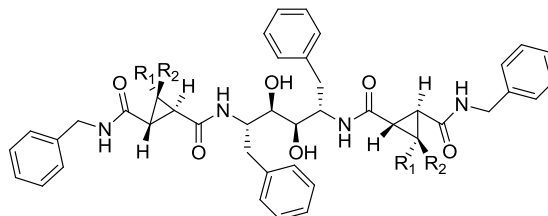


**Figure 14: Intramolecular cyclopropanation using a rhodium catalyst**

Knowledge of the HIV-protease active-site led Martin, *et al.* to explore integration of cyclopropane rings in a known, highly potent inhibitor **20** (Figure 15).<sup>115</sup> Using the intramolecular cyclopropanation synthesis, methyl group incorporation as substituents on the cyclopropane ring was evaluated. The constrained core of compounds **21-24** gave a pre-determined orientation of side chains found to be biologically active for the HIV-protease enzyme and equivalent in potency to compound **20**.<sup>109</sup> The use of the cyclic derivatives as rigid replacement options were accepted by the HIV-protease enzyme active site. Extensive X-ray crystal structure data revealed the cyclopropane-derived inhibitor **22** bound to the active-site of HIV-protease similarly to lead compound **20**, which contains the more flexible peptide core.<sup>109</sup>



Compound 20



Compound 21:  $R_1 = R_2 = \text{CH}_3$   
 Compound 22:  $R_1 = \text{CH}_3, R_2 = \text{H}$   
 Compound 23:  $R_1 = \text{H}, R_2 = \text{CH}_3$   
 Compound 24:  $R_1 = R_2 = \text{H}$

**Figure 15: Cyclopropane-derived HIV-1 protease inhibitors**

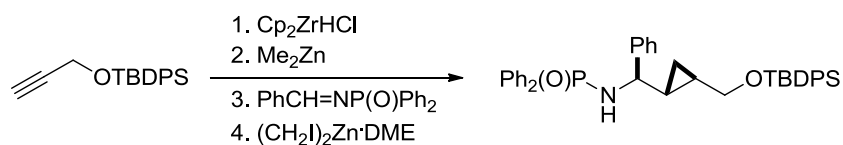


**Figure 16: Multi-component condensation cyclopropanation synthesis**

Multi-component condensation reactions of organozirconocene, aldimine and zinc carbenoid were used by Wipf, *et al.* to synthesize stereoselective cyclopropane-derived peptides (Figure 16).<sup>116-118</sup> The C- and N-termini were diversified from the phenylglycine backbone to create a library of 46 compounds for development of a structure-activity relationship profile.<sup>118</sup> Another approach used by Wipf was the

combination of a water-accelerated methylalumination reaction with a Simmons-Smith cyclopropanation (Figure 17) to synthesize a protected cyclopropylalkylamide compound **25**<sup>117</sup>; used as an intermediate to form enantiomerically pure derivatives. One such derivative, compound **26** (Figure 18), was shown by X-ray crystal structure analysis to control secondary structure features, a concept important in the use of cyclopropane-derived peptidomimetics.

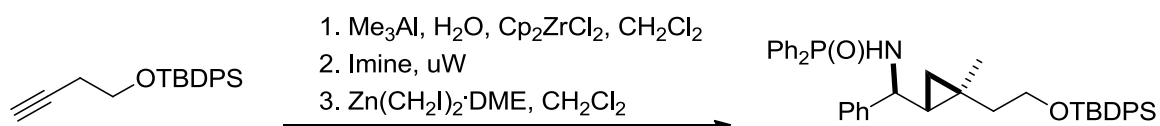


**Figure 17: Simmons-Smith cyclopropanation**

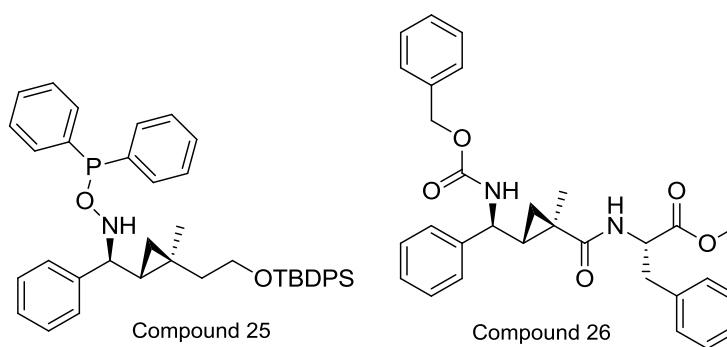


**Figure 18: Wipf's cyclopropyl peptide isosteres**

*The Dunlap Laboratory Approach.* The Dunlap laboratory has developed an efficient method to form the hydroxyethylene cyclopropyl core of peptidomimetic structures (Figure 19).<sup>119</sup> The desired cyclopropyl backbone was synthesized in three steps with the use of the stabilized sulfur ylide EDSA, followed by ketone reduction. As shown in Figure 19, this approach converted the commercially available Cbz-protected amino acids to the corresponding Weinreb amides followed by the addition of vinylmagnesium bromide to afford the enones, which were subjected to cyclopropanation using EDSA. After ketone reduction, the Cbz-protected cyclopropane-derived peptidomimetic core was synthesized in good yields. Although extensive stereochemical analysis has been performed, the ability to recover multiple isomers may prove beneficial when establishing enzymatic inhibition. Five amino acid series have been completed thus far.<sup>119</sup>

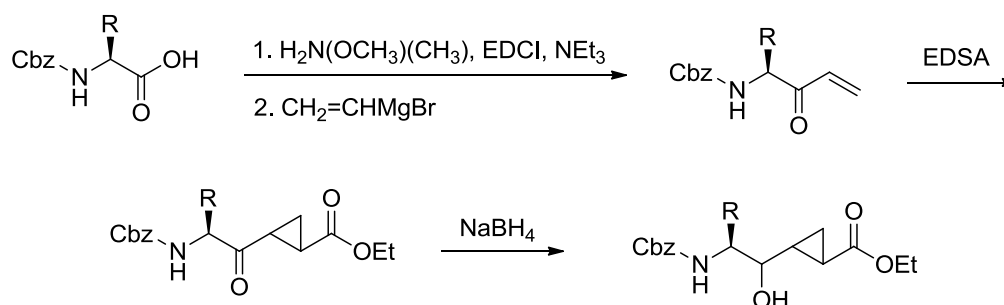


**Figure 19: The Dunlap laboratory cyclopropyl peptidomimetic synthesis**

*Nitrocyclopropanation.* The synthesis of the substituted enone creates access to positioning of the nitrogen of the amide adjacent to the cyclopropyl ring (reverse amide). Making use of a Curtius rearrangement would afford the reverse amide from the acid, however a more efficient approach would be to incorporate the nitrogen in the cyclopropanation step of the peptidomimetic synthesis (Figure 20).<sup>120</sup> Similar to the EDSA cyclopropanation, nitrocyclopropanation using bromonitromethane has been used in other syntheses.<sup>121-123</sup> The Dunlap laboratory is the first to use the nitrocyclopropanation to synthesize a variety of cyclopropane-derived peptidomimetic structures to be used as intermediates for potential biologically active compounds.<sup>120</sup>

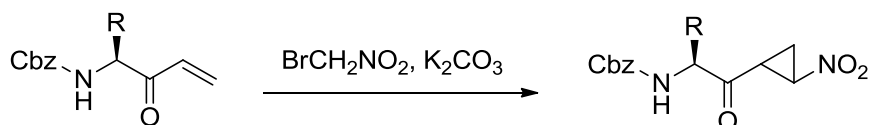


**Figure 20: Nitrocyclopropanation using bromonitromethane**

### Objective.

A series of leucine cyclopropane-derived peptidomimetics, as potential BACE inhibitors, will be synthesized using the nitrocyclopropanation approach developed in the Dunlap laboratory. The main focus of this thesis project was to reduce the nitro group and remove the Cbz-protecting group to make both amines available for coupling reactions. Transfer hydrogenation or Raney nickel was used to synthesize the unstable

di-amine to be characterized as the di-acetate. The Cbz-protecting group was removed by hydrogenation or transfer hydrogenation followed by coupling to benzoic acid or a known active BACE side chain, N-dipropyl isophthalamide.

## CHAPTER II: MATERIALS AND METHODS

Synthesis of the cyclopropyl peptidomimetic compounds began with commercially available N-(carbobenzyloxy)-L-leucine **27** which was then converted to the known N-methoxy-N-methylamide (Weinreb amide) **28**. A terminal enone **29** was formed from the Weinreb amide by a Grignard addition of vinylmagnesium bromide. Nitrocyclopropanation of the enone afforded the cyclopropyl nitro ketone **30**. Using sodium borohydride, the ketone of **30** was reduced to the alcohol **31**. Synthesis of the Cbz-L-leucine cyclopropyl nitro alcohol is shown in Figure 21.

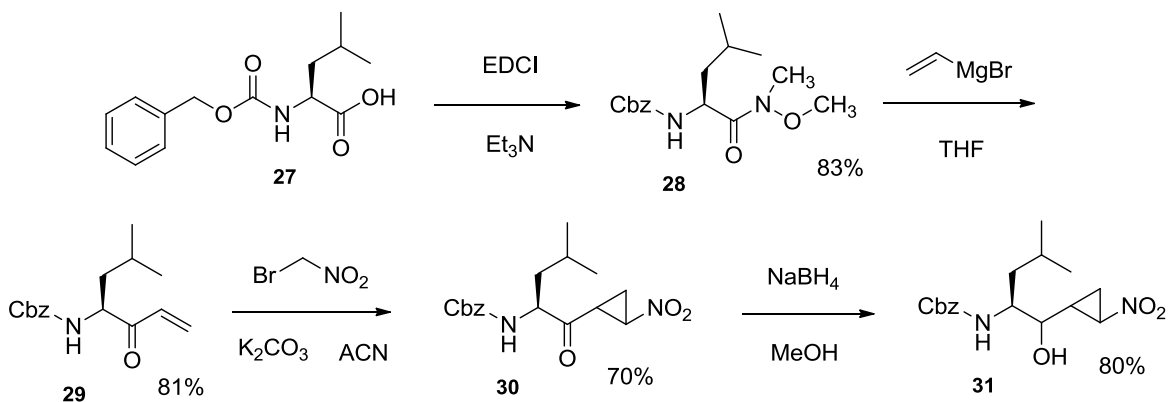


**Figure 21: Synthesis of Cbz-leucine cyclopropyl nitro alcohol**

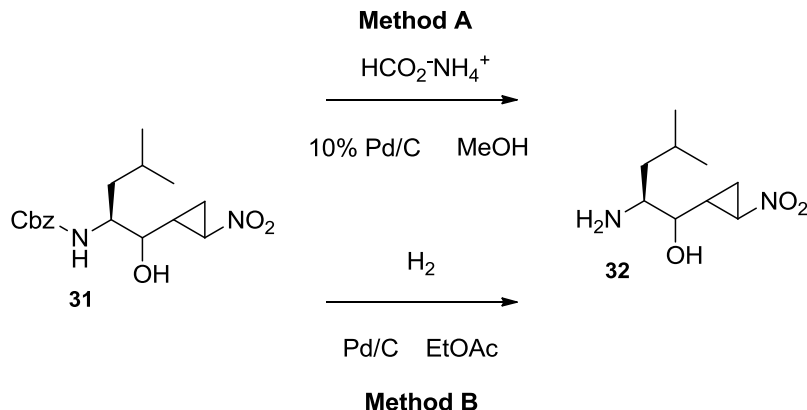


**Figure 22: Reduction of the Cbz protecting group**

Transfer hydrogenation with ammonium formate and Pd/C for five hours (Method A) or an overnight hydrogenation (Method B) removed the Cbz protecting group (deprotection) to form the nitro-mono-amine **32** (Figure 22). Coupling of the mono-amine **32** to the BACE side chain, 3-(dipropylcarbamoyl)benzoic acid **33** or benzoic acid using EDCI and HOBT or COMU, was expected to afford the nitro amide **34** or **35** (Figure 23 and 24). A 48 hour transfer hydrogenation removed the Cbz and reduced the nitro to afford the unstable di-amine **36**, which was quickly converted to the di-acetate **37** for characterization (Figure 25). No attempt was made to separate diastereomers at any stage in the synthesis, although the *syn* and *anti* isomers of the nitro ketone **30** have been purified for characterization purposes.

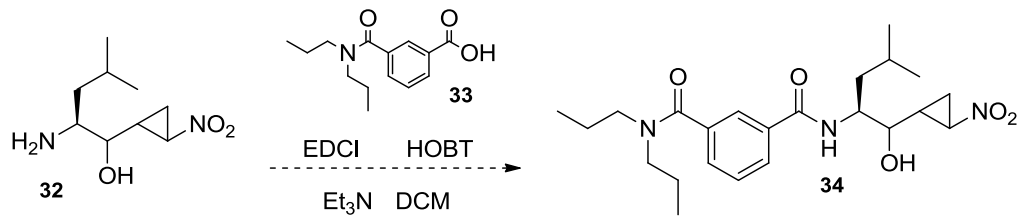


**Figure 23: BACE side chain coupling reaction**

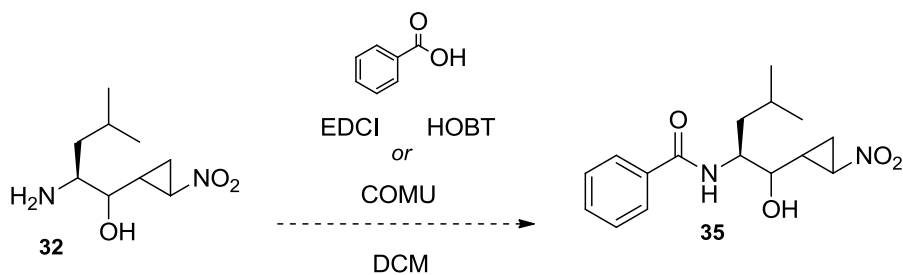


**Figure 24: Benzoic acid coupling reaction**

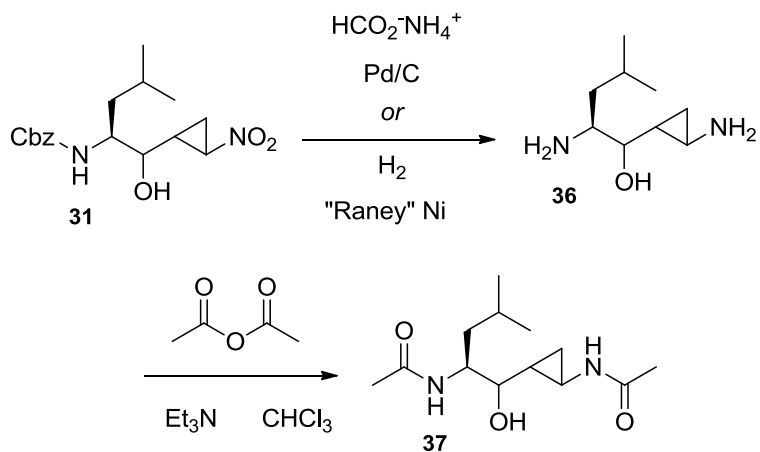


**Figure 25: Unstable di-amine synthesis**

## Instruments, Materials, and Reagents

The NMR data were obtained by using a 500 MHz FT-NMR model ECA-500 JEOL (Peabody, MA) purchased with funding provided by the National Science Foundation through the NSF-RUI program (#0321211) and where indicated a DRX 400 MHz Bruker (The Woodlands, TX). Chemical shifts are reported in parts per million using tetramethylsilane (TMS) as an internal reference. Splitting patterns are designated by the following: s (singlet), d (doublet), t (triplet), q (quartet), m (multiplet), and dd (doublet of doublets). High resolution electrospray ionization-mass spectrometry (ESI-MS) was performed at Notre Dame University, Notre Dame, Indiana.

Thin layer chromatography (TLC) was performed on glass plates coated with silica gel and UV active backing purchased from Fisher Scientific, Pittsburgh, PA. The TLC plates were analyzed with a short wavelength (254 nm) UV light and subsequently stained with phosphomolybdic acid (reagent grade, Aldrich, Milwaukee, WI) prepared as a 10% solution in ethanol. Column chromatography was performed with silica gel, 60 Å 230-400 mesh ASTM (reagent grade, Fisher Scientific, Pittsburgh, PA) and flash chromatography was performed on an ISCO CombiFlash R<sub>f</sub> 200 (Teledyne ISCO, Lincoln, NE).

Methylene chloride, methanol, acetone, acetonitrile, ethyl acetate and hexanes were purchased from Fisher Scientific, Pittsburgh, PA. Chloroform was purchased reagent grade from Acros Organic, New Jersey, USA. Deutero-chloroform (CDCl<sub>3</sub>) was purchased from Aldrich, Milwaukee, WI and Cambridge Isotope Laboratories, Inc.,

Andover, MA. Solvent extractions were performed using ethyl acetate or methylene chloride where indicated and washed with 1M HCl, saturated sodium bicarbonate, and brine (reagent grade, Fisher Scientific, Pittsburgh, PA). The organic layer was dried with magnesium sulfate (Fisher Scientific, Pittsburgh, PA) and filtered. Evaporation of solvents was achieved using a Buchi rotary evaporator (Model RII, Buchi, Switzerland) or Heidolph rotary evaporator (Model Hei-VAP Value/G5, Heidolph, Germany).

Triethylamine (Et<sub>3</sub>N) was obtained from Fisher Scientific, Pittsburgh, PA. Anhydrous reagent grade vinylmagnesium bromide and tetrahydrofuran (THF) were purchased from Aldrich, Milwaukee, WI. Other reagents including N-(carbobenzyloxy)-L-leucine, N,O-dimethyl hydroxylamine hydrochloride, N-(3-dimethylaminopropyl)-N'-ethylcarbodiimide hydrochloride (EDCI), hydroxybenzotriazole (HOBT), bromonitromethane, potassium carbonate, sodium borohydride, 10% palladium on carbon, Raney®-Nickel, slurry in H<sub>2</sub>O, active catalyst, and ammonium formate were obtained from Aldrich, Milwaukee, WI. BACE side chain **33** was prepared as reported in the literature.<sup>125</sup>

## Synthetic Methods

**(S)-Benzyl (1-(methoxy(methyl)amino)-4-methyl-1-oxopentan-2-yl)carbamate (28)**. To a solution of N-(carbobenzyloxy)-L-leucine **27** (1.5 g, 5.6 mmol) in 15 mL methylene chloride, was added N,O-dimethyl hydroxylamine hydrochloride (550 mg, 5.6 mmol), followed by N-(3-dimethylaminopropyl)-N'-ethylcarbodiimide hydrochloride (EDCI) (1.09 g, 5.6 mmol), and triethylamine (Et<sub>3</sub>N) (790 μL, 5.6 mmol)

after 10 minutes. The solution was allowed to stir overnight at room temperature. After diluting the reaction with 80 mL ethyl acetate, the solution was washed with 1M HCl, aqueous sodium bicarbonate and water. The organic layer was dried with magnesium sulfate, filtered, and solvent was evaporated. The crude product was chromatographed on 25 x 100 mm silica gel eluting sequentially with 1:6, 1:4, and 1:2 ethyl acetate-hexane to afford 1.31 g (75.5%) of the Weinreb amide **28**.

$^1\text{H-NMR}$  (500 MHz,  $\text{CDCl}_3$ ):  $\delta$  7.32-7.28 (m, 5 aryl  $\text{CH}$ ), 5.48 (d, 1H,  $J=9.2$ ,  $\text{NH}$ ), 5.07(dd, 2H,  $J=12.60\text{Hz}$ ,  $\text{CH}_2\text{CBz}$ ), 4.7 (m, 1H,  $\text{CH}$ ), 3.76 (s, 3H,  $\text{OCH}_3$ ), 3.16 (s, 3H,  $\text{NCH}_3$ ), 1.71 (m, 1H,  $\text{CH}(\text{CH}_3)_2$ ), 1.44 (dd, 2H,  $J=7.16$ ,  $\text{CH}$ ), 0.90 (d, 3H,  $J=6.87$ ,  $\text{CH}_3\text{CH}$ ), 0.86 (d, 3H,  $J=6.30$ ,  $\text{CH}_3\text{CH}$ );  $^{13}\text{C-NMR}$  (125 MHz,  $\text{CDCl}_3$ ):  $\delta$  170.2 (ester  $\text{C=O}$ ), 156.2 ( $\text{CBz C=O}$ ), 136.4 ( $4^\circ$  aryl  $\text{C}$ ), 128.3-127.8 (6 aryl  $\text{C}$ 's), 66.1 ( $\text{CH}_2\text{CBz}$ ), 61.4 ( $\text{OCH}_3$ ), 49.4 ( $\text{CHN}$ ), 41.75 ( $\text{CH}_2$ -isobutyl), 24.54 ( $\text{CH}(\text{CH}_3)_2$ ), 23.19 ( $\text{CH}_3$ 's).

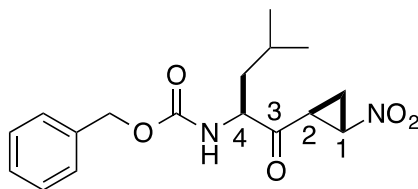
**(S)-Benzyl (6-methyl-3-oxohept-1-en-4-yl)carbamate (29)**. The Weinreb amide **28** (1.31 g, 4.25 mmol) was dissolved in 10.6 mL THF and cooled to  $0^\circ\text{C}$  under argon. Vinylmagnesium bromide (10.6 mL of 1M solution, 10.6 mmol) was added and the reaction was allowed to warm up to room temperature and stir for three hours. The solution was diluted with ethyl acetate and the organic layer was washed with 1M HCl, and aqueous sodium bicarbonate. The organic layer was dried with magnesium sulfate, filtered, and solvent was evaporated. The crude product was chromatographed on 25 x 100 mm silica gel eluting with 1:10 ethyl acetate-hexane to afford 950 mg (81.2%) of the enone **29**.

$^1\text{H-NMR}$  (500 MHz,  $\text{CDCl}_3$ ):  $\delta$  7.33-7.25 (m, 5H, aryl), 6.45 (dd,  $J = 10.3, 17.1$ , 1H, vinyl C2H), 6.39 (d, 2H,  $J=17.0$ , C1H *trans*), 5.87 (d, 2H,  $J=10.3$ , C1H *cis*), 5.50 (d, 1H,  $J=8.02\text{Hz}$ , NH), 5.08 (s, CH<sub>2</sub> CBz), 4.27 (m, CHN), 1.71 (m, CH), 1.38 (dd, CH), 0.98 (d, 3H,  $J=6.87\text{Hz}$ , CH<sub>3</sub>CH), 0.90 (d, 3H,  $J=6.87\text{Hz}$ , CH<sub>3</sub>CH<sub>4</sub>);  $^{13}\text{C-NMR}$  (125 MHz,  $\text{CDCl}_3$ ):  $\delta$  198.7 (ketone), 156.0 (CBz C=O), 135.6 (4° aryl C), 130.0 (CH alkene), 128.4 (CH<sub>2</sub> alkene), 128.4-127.9 (3 aryl), 66.8 (CH<sub>2</sub>CBz), 56.1 (CHN), 41.4 (CH<sub>2</sub> isobutyl), 24.7 (CH isobutyl), 23.2 (CH<sub>3</sub>), 21.7 (CH<sub>3</sub>); mass spectrum (ESI-MS)  $m/z$  ( $\text{C}_{16}\text{H}_{22}\text{NO}_5$ ) calculated for (M+1) 276.1594, found 276.1600.

**Benzyl ((2S)-4-methyl-1-(2-nitrocyclopropyl)-1-oxopentan-2-yl)carbamate**

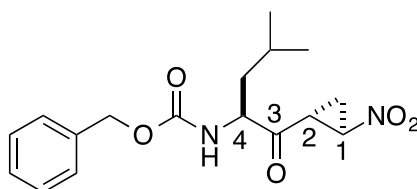
**(30)**. To a solution of enone **29** (1.44 g, 5.24 mmol) in 10 mL acetonitrile set on ice was added freshly ground potassium carbonate (867 mg, 6.28 mmol) and bromonitromethane (438  $\mu\text{L}$ , 6.28 mmol). The solution was allowed to warm to room temperature and stir for six hours. At hour two and four, more bromonitromethane (438  $\mu\text{L}$ , 6.28 mmol) was added. The reaction was diluted with ethyl acetate and the organic layer was washed with water and brine. The organic layer was dried with magnesium sulfate, filtered, and solvent was evaporated. Purification by flash chromatography on silica gel afforded 1.3 g (74%) of the nitrocyclopropyl ketone **30**. Exact mass spectrum (ESI-MS)  $m/z$  ( $\text{C}_{17}\text{H}_{22}\text{N}_2\text{O}_5$ ) calculated for (M+1) 335.1601. Found 335.1561.

The isomers were separated by HPLC with an initial solvent ratio of 70/30 hexane-ethyl (3.0 min), to 60/40 over 10.0 min. (hold for 5 min), to 55/45 over 6.0 min., holding for 2.0 min. for a total run time of 26.0 min with a flow rate of 2.0 mL/min. Peaks integrated to a 1.8:1.0 ratio.



**Benzyl ((S)-4-methyl-1-((1S,2S)-2-nitrocyclopropyl)-1-oxopentan-2-**

**yl)carbamate (*syn*-30).** RT = 13.6 min.  $[\alpha]_D = +250.2^\circ$   $^1\text{H-NMR}$  ( $\text{CDCl}_3$ , 500 MHz):  $\delta$  7.36-7.25 (m, 5H, aryl CH), 5.18 (d,  $J = 7.45$ , 1H, NH), 5.10 (s, 2H,  $\text{CH}_2\text{Cbz}$ ), 4.59-4.56 (m, 2H, C1H and C4H), 3.09 (m, 1H, C2H), 2.06, 1.71 (m, each 1H,  $\text{CH}_2\text{cpyl}$ ), 1.66-1.52 (m, 2H,  $\text{CH}_2\text{CH}(\text{CH}_3)_2$ ), 1.41 (m, 1H,  $\text{CH}_2\text{CH}(\text{CH}_3)_2$ ), 1.00 (d,  $J = 6.3$  Hz, 3H,  $(\text{CH}_3)$ ), 0.96 (d,  $J = 6.8$  Hz, 3H,  $\text{CH}_3$ );  $^{13}\text{C-NMR}$  ( $\text{CDCl}_3$ , 125 MHz):  $\delta$  204.0 (ketone  $\text{C}=\text{O}$ ), 156.1 (Cbz  $\text{C}=\text{O}$ ), 136.08 ( $4^\circ$  aryl C), 128.70-128.27 (5 aryl C's), 67.41 ( $\text{CH}_2\text{Cbz}$ ), 65.72 (C1), 59.44 (C4), 40.02 ( $\text{CH}_2\text{CH}(\text{CH}_3)_2$ ), 28.63 (C2), 24.94 ( $\text{CH}(\text{CH}_3)_2$ ), 23.31 ( $\text{CH}_3$ ), 21.72 ( $\text{CH}_3$ ), 19.17 ( $\text{CH}_2$  cpyl).



**Benzyl ((S)-4-methyl-1-((1R,2R)-2-nitrocyclopropyl)-1-oxopentan-2-**

**yl)carbamate (*anti*-30).** RT = 14.3 min.  $[\alpha]_D = +27.64^\circ$ .  $^1\text{H-NMR}$  ( $\text{CDCl}_3$ , 500 MHz):  $\delta$  7.36-7.25 (m, 5H, aryl CH), 5.21 (d, 1H, NH), 5.10 (s, 2H,  $\text{CH}_2\text{Cbz}$ ), 4.55 (m, 2H, C1H and C4H), 3.08 (m, 1H, C2H), 2.07, 1.73 (m, each 1H,  $\text{CH}_2\text{cpyl}$ ), 1.66-1.52 (m, 2H,  $\text{CH}_2\text{CH}(\text{CH}_3)_2$ ), 1.42 (m, 1H,  $\text{CH}_2\text{CH}(\text{CH}_3)_2$ ), 0.99 (d,  $J = 6.3$  Hz, 3H,  $(\text{CH}_3)$ ), 0.95 (d,  $J =$

6.8Hz, 3H, CH<sub>3</sub>); <sup>13</sup>C-NMR (CDCl<sub>3</sub>, 125 MHz): δ 204.0 (ketone C=O), 156.1 (Cbz C=O), 136.08 (4° aryl C), 128.70-128.27 (5 aryl C's), 67.41 (CH<sub>2</sub>Cbz), 65.72 (C1), 59.34 (C4), 39.93 (CH<sub>2</sub>CH(CH<sub>3</sub>)<sub>2</sub>), 28.63 (C2), 24.94 (CH(CH<sub>3</sub>)<sub>2</sub>), 23.31 (CH<sub>3</sub>), 21.72 (CH<sub>3</sub>), 19.17 (CH<sub>2</sub> cpyl).

**Benzyl ((2*S*)-1-(2-nitrocyclopropyl)-1-hydroxy-4-methylpentan-2-yl)carbamate (31).** To a solution of ketone **30** (203 mg, 0.61 mmol) in 17 mL of methanol was added sodium borohydride (115 mg, 3.30 mmol) for three hours and then poured into ethyl acetate and washed with water and brine. The organic layer was dried over magnesium sulfate, filtered, and the solvent was evaporated. The crude product was chromatographed on 25 x 100 mm silica gel eluting sequentially with 1:6, 1:3, and 1:1 ethyl acetate-hexane to afford 163 mg (80%) of the alcohol **31** as a mixture of isomers.

<sup>1</sup>H-NMR (CDCl<sub>3</sub>, 400 MHz): δ 7.38-7.28 (m, 5H, aryl CH), 5.12 (s, 2H, CH<sub>2</sub>Cbz), 4.85 (d, J = 5.92 Hz, 1H, NH), 3.82 (s, 1H, OH), 3.72-3.69 (m, 1H, C4H), 3.58-3.54 (m, 1H, C2H), 2.07, 0.09 (s, 1H each, CH<sub>2</sub>cpyl), 1.72-1.65 (m, 1H, CH<sub>2</sub>CH(CH<sub>3</sub>)<sub>2</sub>), 1.39-1.34 (m, 2H, CH<sub>2</sub>CH(CH<sub>3</sub>)<sub>2</sub>), 0.96 (d, J = 6.52 Hz, 6H, (CH<sub>3</sub>)<sub>2</sub>); <sup>13</sup>C-NMR (CDCl<sub>3</sub>, 125 MHz): δ 157.77 (Cbz C=O), 136.01 (4° aryl C), 128.73-128.27 (5 aryl C's), 77.36 (CHOH (C3)) 71.43 (CH<sub>2</sub>Cbz), 67.57 (C1), 54.72 (C4), 39.36 (CH<sub>2</sub>CH(CH<sub>3</sub>)<sub>2</sub>), 26.41 (C2), 24.79 (CH(CH<sub>3</sub>)<sub>2</sub>), 23.45 (CH<sub>3</sub>), 21.68 (CH<sub>3</sub>), 14.26 (CH<sub>2</sub> cpyl). Mass spectrum (ESI-MS) *m/z* (C<sub>17</sub>H<sub>25</sub>N<sub>2</sub>O<sub>5</sub>) calculated for (M+1) 337.1745. Found 337.1758.

**(2*S*)-2-Amino-4-methyl-1-(2-nitrocyclopropyl)pentan-1-ol (32). Method A:** To a solution of N-Cbz-l-leucine-alcohol **31** (34 mg, 0.101 mmol) in 5 mL of methanol (HPLC grade) was added ammonium formate (160 mg, 2.53 mmol) and 10% palladium

on carbon (30 mg). After stirring for five hours, the catalyst was filtered through Celite and washed with methylene chloride and water. The organic layer was extracted with water twice. The aqueous layer was lyophilized to afford the unstable mono-amine **32** (reduction of Cbz).

<sup>1</sup>H-NMR (CDCl<sub>3</sub>, 400 MHz): δ 5.34 (m, 2H, NH<sub>2</sub>), 4.12 (d, J = 19.32, 1H, C1H), 3.81 (s, 1H, OH), 3.74 (s, 1H, C3H), 3.43-3.38 (m, 1H, C4H), 3.08 (s, 1H, C2H), 2.05, 1.93 (s, each 1H, CH<sub>2</sub>cpyl), 1.73-1.64 (m, 1H, CH<sub>2</sub>CH(CH<sub>3</sub>)<sub>2</sub>), 1.40-1.32 (m, 2H, CH<sub>2</sub>CH(CH<sub>3</sub>)<sub>2</sub>), 0.93-0.89 (m, 6H, (CH<sub>3</sub>'s)). Mass spectrum (ESI-MS) *m/z* (C<sub>9</sub>H<sub>18</sub>N<sub>2</sub>O<sub>3</sub>) calculated for (M+1) 203.1390. Found 203.1413.

**(2S)-2-Amino-4-methyl-1-(2-nitrocyclopropyl)pentan-1-ol (32). Method B:**

To a solution of N-Cbz-l-leucine-alcohol **31** (122 mg, 0.363 mmol) in 25 mL ethyl acetate was added a mass equal amount of 10% palladium on carbon. The solution was set on the Parr shaker at 40 psi for 18 hours. The solution was filtered over Celite, filtered again, and washed well with ethyl acetate. The solvent was evaporated to afford 70 mg (96%) of the mono-amine **32** (reduction of Cbz).

<sup>1</sup>H-NMR (CDCl<sub>3</sub>, 400 MHz): δ 5.34 (m, 2H, NH<sub>2</sub>), 4.12 (d, J = 19.32, 1H, C1H), 3.81 (s, 1H, OH), 3.74 (s, 1H, C3H), 3.43-3.38 (m, 1H, C4H), 3.08 (s, 1H, C2H), 2.05, 1.93 (s, each 1H, CH<sub>2</sub>cpyl), 1.73-1.64 (m, 1H, CH<sub>2</sub>CH(CH<sub>3</sub>)<sub>2</sub>), 1.40-1.32 (m, 2H, CH<sub>2</sub>CH(CH<sub>3</sub>)<sub>2</sub>), 0.93-0.89 (m, 6H, (CH<sub>3</sub>'s)). Mass spectrum (ESI-MS) *m/z* (C<sub>9</sub>H<sub>18</sub>N<sub>2</sub>O<sub>3</sub>) calculated for (M+1) 203.1390. Found 203.1402.

**N1-((2S)-1-hydroxy-4-methyl-1-(2-nitrocyclopropyl)pentan-2-yl)-N3, N3-dipropylisophthalamide (34).** To a solution of mono-amine **32** (70 mg, 0.347 mmol) in

2 mL dichloromethane was added a solution of 3-(dipropylcarbamoyl)benzoic acid (104 mg, 0.416 mmol), 1-ethyl-3-(3-dimethylaminopropyl)carbodiimide (EDCI, 80 mg, 0.416 mmol), hydroxybenzotriazole (HOBT, 56 mg, 0.416 mmol), and Et<sub>3</sub>N (58  $\mu$ L, 0.416 mmol) in 1 mL dichloromethane. After stirring overnight, the solution was diluted with dichloromethane. The organic layer was washed with water and dried over magnesium sulfate, filtered, and the solvent was evaporated. Purification by flash chromatography on silica gel afforded 44.4 mg (36%) of an undetermined coupling product **34**.

<sup>1</sup>H-NMR (CDCl<sub>3</sub>, 400 MHz):  $\delta$  8.03-7.34 (m, 5H, aryl), 6.66 (d, J = 8.64, 1H, NH), 4.63 (d, J = 4.8, 1H, OH), 3.45 (s, 2H, CH<sub>2</sub>propylN), 3.13 (s, 2H, CH<sub>2</sub>propyl), 0.99-0.87 (dd, J = 6.52, J = 6.2, 6H, (CH<sub>3</sub>)<sub>2</sub>isobutyl). C-NMR (CDCl<sub>3</sub>, 125 MHz):  $\delta$  165.07 (BACEC=O), 158.87 (amideC=O), 132.44-127.58 (4 aryl C's), 66.7 (CH<sub>2</sub>N or CH<sub>2</sub>O).

**N-((2S)-1-hydroxy-4-methyl-1-(2-nitrocyclopropyl)pentan-2-yl)benzamide (35)**. To a solution of mono-amine **32** (40 mg, 0.198 mmol) in 2 mL dichloromethane was added a solution of benzoic acid (29 mg, 0.238 mmol), 1-ethyl-3-(3-dimethylaminopropyl)carbodiimide (EDCI, 46 mg, 0.238 mmol), hydroxybenzotriazole (HOBT, 32 mg, 0.238 mmol), and Et<sub>3</sub>N (33  $\mu$ L, 0.238 mmol) in 1 mL dichloromethane. After stirring overnight, the solution was diluted with dichloromethane. The organic layer was washed with water and dried over magnesium sulfate, filtered, and the solvent was evaporated. Purification by flash chromatography on silica gel afforded 10 mg (17%) of an undetermined coupling product **35**.

$^1\text{H-NMR}$  ( $\text{CDCl}_3$ , 400 MHz):  $\delta$  8.10-7.44 (m, 5H, aryl), 6.28 (d,  $J = 6.68$ , 1H, NH), 4.63 (m, 1H, OH), 1.01-0.95 (m, 6H,  $(\text{CH}_3)_2$ isobutyl).  $\text{C-NMR}$  ( $\text{CDCl}_3$ , 125 MHz):  $\delta$  158.87 (amide  $\text{C}=\text{O}$ ), 132.44-127.58 (4 aryl C's), 66.7 ( $\text{CH}_2\text{N}$  or  $\text{CH}_2\text{O}$ ).

**N-((2S)-1-hydroxy-4-methyl-1-(2-nitrocyclopropyl)pentan-2-yl)benzamide**

**(35).** To a solution of mono-amine **32** (72 mg, 0.356 mmol) in 5 mL dichloromethane was added benzoic acid (43.5 mg, 0.356 mmol), (1-cyano-2-ethoxy-2-oxoethylideneaminoxy)dimethylamino-morpholino-carbenium hexafluorophosphate (COMU, 229 mg, 0.535 mmol), and diisopropylethylamine (DIEA, 93  $\mu\text{L}$ , 0.535 mmol). After stirring overnight, the solution was diluted with ethyl acetate. The organic layer was washed with 1M HCl, brine, and saturated sodium bicarbonate. After dried over magnesium sulfate and filtered, the solvent was evaporated. Purification by flash chromatography on silica gel afforded 33 mg (30%) of an undetermined coupling product **35**.

$^1\text{H-NMR}$  ( $\text{CDCl}_3$ , 400 MHz):  $\delta$  8.12-7.43 (m, 5H, aryl), 6.29 (d,  $J = 6.76$ , 1H, NH), 4.32 (m, 1H, OH), 1.01-0.95 (m, 6H,  $(\text{CH}_3)_2$ isobutyl).  $\text{C-NMR}$  ( $\text{CDCl}_3$ , 125 MHz):  $\delta$  158.87 (amide  $\text{C}=\text{O}$ ), 132.44-127.58 (4 aryl C's), 66.7 ( $\text{CH}_2\text{N}$  or  $\text{CH}_2\text{O}$ ).

**(2S)-2-Amino-1-(2-aminocyclopropyl)-4-methylpentan-1-ol (36).** To a solution of N-Cbz-l-leucine-alcohol **31** (17 mg, 0.05 mmol) in 5 mL of methanol (HPLC grade) was added ammonium formate (80 mg, 1.25 mmol) and 10% palladium on carbon (30 mg). After stirring for 48 hours, the catalyst was filtered through Celite and washed with methylene chloride. The organic layer was extracted with water twice. The aqueous layer was lyophilized to afford the unstable di-amine **36**.

$^1\text{H-NMR}$  ( $\text{D}_2\text{O}$ , 300 MHz):  $\delta$  3.48 (dd,  $J = 3.45, 3.42$ , 1H, C1H), 3.36-3.29 (m, 1H, OH), 3.21-3.14 (m, 1H, C3H), 2.98 (dd,  $J = 6.51, 4.83$ , 1H, C4H), 2.57-2.47 (m, 1H, C2H), 1.6-1.2 (m, 2H,  $\text{CH}_2\text{CH}(\text{CH}_3)_2$ ), 0.98 (m, 1H,  $\text{CH}_2\text{CH}(\text{CH}_3)_2$ ), 0.89 (m, 2H,  $\text{CH}_2$  cpyl), 0.80-0.75 (dd,  $J = 4.44, 5.16$ , 6H,  $\text{CH}_3$ 's). Mass spectrum (ESI): 173 (M+H), 158 (M-15).

**(2S)-2-Amino-1-(2-aminocyclopropyl)-4-methylpentan-1-ol (36).** To a solution of N-Cbz-l-leucine-alcohol **31** (30 mg, 0.089 mmol) in 5 mL methanol (HPLC grade) was added a catalytic amount of "Raney" nickel, while being flushed with argon. Under hydrogen gas at one atmosphere, the reaction was stirred, vigorously, for 18 hours. The solution was filtered over Celite and washed well with 3:1 chloroform/isopropanol solution. The solvent was evaporated to afford the unstable di-amine **36**.

**N-(2-((2S)-2-acetamido-1-hydroxy-4-methylpentyl)cyclopropyl)acetamide (37).** To a solution of the di-amine **35** (17 mg, 0.093 mmol) in 1 mL of chloroform was added acetic anhydride (88  $\mu\text{L}$ , 0.93 mmol) and triethylamine (130  $\mu\text{L}$ , 0.93 mmol). After the reaction stirred for 18 hours, water was added and the product was extracted using ethyl acetate. The organic layer was washed twice with water before being dried with magnesium sulfate. The solvent was evaporated to afford the di-acetate **37**.

$^1\text{H-NMR}$  ( $\text{CDCl}_3$ , 400 MHz):  $\delta$  5.48 (d,  $J = 8.32$  Hz, NH), 4.32-4.28 (m, 1H, C4H), 4.16-4.02 (m, 3H, C1H, C2H, C3H), 2.23, 2.08, 2.06, 1.99 (4s, acetate  $\text{CH}_3$ 's), 1.67-1.61 (m, 2H,  $\text{CH}_2$  cpyl), 1.44-1.27 (m, 3H,  $\text{CH}_2\text{CH}$ ), 0.96-0.93 (dd,  $J = 3.76, 3.64$ , 6H,  $\text{CH}_3$ 's).

### CHAPTER III: RESULTS AND DISCUSSION

Using the cyclopropyl approach developed in the Dunlap laboratory (see Figure 19), five amino acids have been converted to the ethyl ester. This key intermediate was used to form final compounds containing the known BACE side chain (Figure 26). From the ethyl ester cyclopropyl, sodium borohydride was used for a ketone reduction followed by hydrogenation to remove the Cbz-protecting group and coupling to the BACE side chain to afford **38**. After hydrolysis of the ethyl ester, the corresponding acid was coupled to various amines in the laboratory to form the standard amide on the right side of the compound **39**. This synthesis has been carried forward with two amino acids, phenyl alanine and leucine, which have been shown to exhibit some bioactivity for inhibition of BACE.

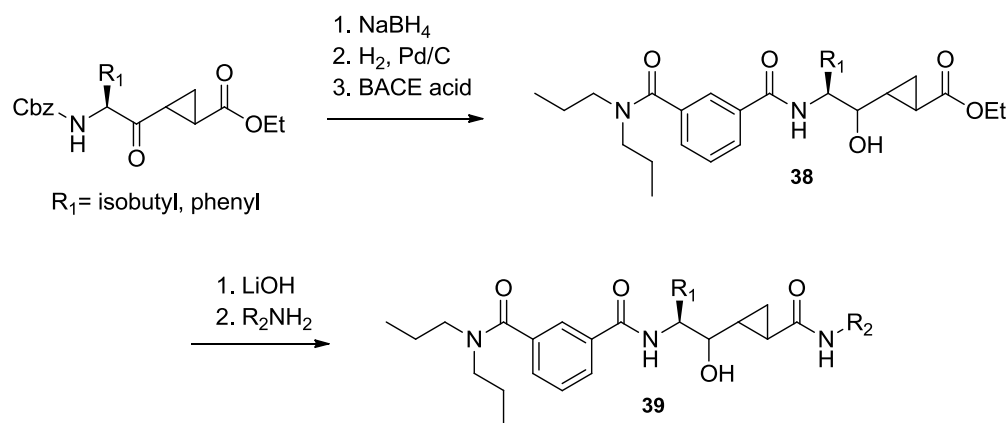


**Figure 26: Ester series amide synthesis**

To further investigate the BACE inhibition activity of these compounds, the nitrocyclopropanation was developed to form the “reverse” amide, with the nitrogen bonded to the cyclopropyl ring rather than the carbonyl. As seen in Figure 21, commercially available Cbz-protected leucine was used to form the terminal enone from the Weinreb amide, which was then subjected to nitrocyclopropanation and ketone reduction to form the key intermediate in the synthesis.

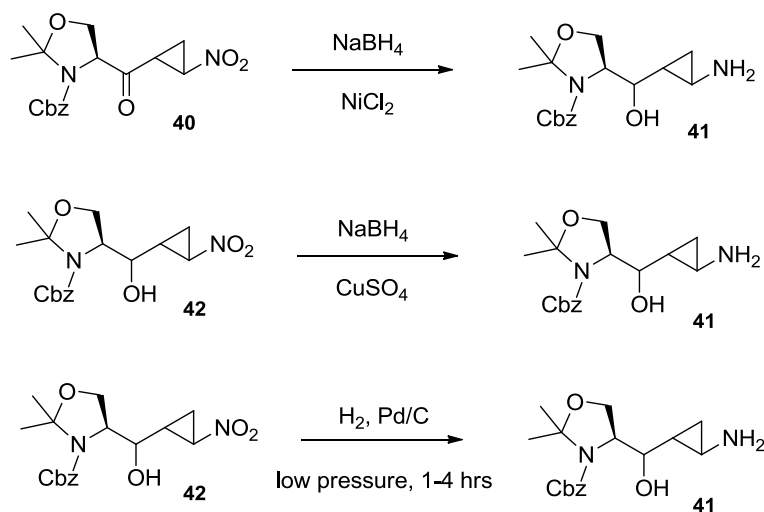


**Figure 27: Previous nitro reduction attempts on serine series**

Reduction of the nitro group is needed in order to form the “reverse” amide. Previous attempts had been made using the nitrocyclopropyl from the serine series. Nitrocyclopropyl ketone **40** was reacted with sodium borohydride and nickel chloride in an attempt to reduce both the alcohol and nitro groups at the same time to form the amino

alcohol **41** (Figure 27). The reaction was unsuccessful, and resulted in decomposition of starting material. The ketone in **40** was reduced successfully with sodium borohydride to form the nitrocyclopropyl alcohol **42**. An attempt to reduce the nitro group using copper sulfate and sodium borohydride again resulted in decomposed starting material. Since standard hydrogenation conditions to remove the Cbz protecting group were 35psi for 18 hours, therefore low pressure conditions were tried for only a few hours. These hydrogenation reactions on **42** yielded only starting material.

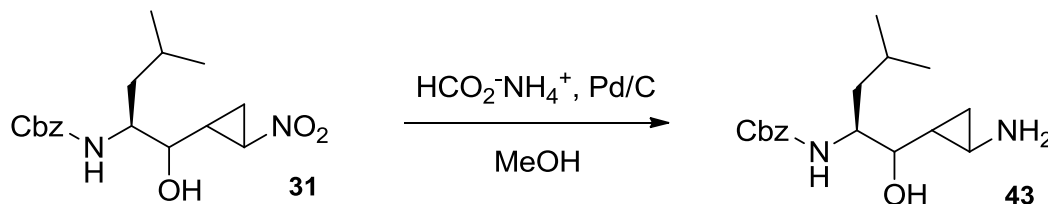


**Figure 28: Transfer hydrogenation desired reaction**

According to reports in the literature, an aliphatic nitro compound can be reduced rapidly using ammonium formate as a catalytic transfer hydrogenation agent.<sup>126-128</sup> Using palladium on carbon and five equivalents of ammonium formate in methanol, the nitro group was expected to be reduced in ten minutes (Figure 28). Transfer hydrogenation attempts are summarized in Table 1. At first attempt there was only unreacted starting material **31** one and a half hours into the reaction. After increasing the amount of ammonium formate to 25 equivalents and letting the reaction stir for three hours, only

undesired product was found in the organic layer. Another attempt was made to heat the reaction to 50°C for 30 minutes, which also proved to be unsuccessful in synthesizing the desired product **43**.

**Table 1: Transfer hydrogenation reaction results**

| Ammonium Formate Equivalents | Time (hrs.) | Reaction Result        |
|------------------------------|-------------|------------------------|
| <b>5</b>                     | 1.5         | Starting material only |
| <b>25</b>                    | 3           | Undesired product      |
| <b>25</b>                    | 0.5 (50°C)  | No product             |
| <b>25</b>                    | 18 (reflux) | No product             |
| <b>25</b>                    | 48          | <b>36</b>              |
| <b>25</b>                    | 5           | <b>32</b>              |

Simultaneously, one reaction was heated at reflux and the other at room temperature overnight. However, at room temperature, after 48 hours, an aminocyclopropane was identified. Since an undesired product had been found previously in the organic layer, the aqueous layer was lyophilized for characterization. From further review of the NMR and exact mass data, it was determined that both the nitro and the Cbz-protecting group had been reduced to form the di-amine **36**. Knowing that the transfer hydrogenation reduced the Cbz protecting group, the reaction was repeated for a shorter time. After analyzing the aqueous layer after transfer

hydrogenation of **31** for five hours, it was found that deprotection occurs before the nitro reduction, forming the mono-amine-nitro **32**.

Removal of the Cbz-protecting group to form the mono-amine-nitro **32** can be carried out by two methods. Transfer hydrogenation using ammonium formate and palladium on carbon for five hours (method A) and hydrogenation at 40 psi for 18 hours (method B) both provide the mono-amine **32**. A transfer hydrogenation for 48 hours or “Raney” nickel reduction for 18 hours forms the di-amine **36**. Stability of the di-amine was uncertain so an acetylation reaction was used to convert the di-amine to the di-acetate **37** for characterization. These conditions allow for selective reduction of the “left side” of the molecule.

Since removal of the Cbz-protecting group preceded nitro reduction, the mono-amine-nitro **32** was used to couple to a known BACE side chain **33** to form the BACE-nitro **34** (Figure 23). This compound was then intended to be subjected to nitro reduction to form the “reverse” amides. Using conditions previously proven successful in the Dunlap laboratory on the ester series, an initial attempt to couple the BACE side chain **33** to the mono-amine-nitro **32** with EDCI and HOBT was attempted. However, the major product was not the desired amide **34**. In the  $^1\text{H}$  NMR, key signals were present including the isobutyl, aryl and N-dipropyl side chains. However, a downfield shift in cyclopropyl signals and a new  $\text{CH}_2$  signal seen in the  $^{13}\text{C}$  NMR, either next to an oxygen or nitrogen, gave suspicions that cyclopropyl ring may have opened.

To eliminate the possibility that the BACE side chain **33** had decomposed by storage over time, the same coupling conditions were used with benzoic acid, instead of

**33**, as a model system to attempt to form the benzoic amide **35** (Figure 24). As with the previous coupling attempt, the exact mass spectrum was not a match, and the  $^1\text{H}$  NMR showed key side chain signals present yet a downfield shift in cyclopropyl signals and a new  $\text{CH}_2$  signal on  $^{13}\text{C}$  NMR. Due to these results, it is proposed that a nucleophile has opened the cyclopropyl ring, which would explain the new  $\text{CH}_2\text{N}$  signal and the downfield shift in the cyclopropyl signals (Figure 29). However, the nucleophile is as yet unidentified, and is not simply the benzoate, based on analysis of the mass spectrum and NMR data.

In response to the failed coupling reactions, a different coupling reagent was used. A coupling attempt using COMU and DIEA to form the benzoic amide **35** afforded very similar results to the EDCI and HOBT coupling reaction. Key  $^1\text{H}$  NMR signals are present including the leucine isobutyl, amide and alcohol protons. The cyclopropyl  $^1\text{H}$  NMR signals are missing and a new  $\text{CH}_2\text{N}$  or  $\text{CH}_2\text{O}$  signal is present as indicated by the  $^{13}\text{C}$  NMR, the same result as with the EDCI coupling. A likely explanation could be that an unknown nucleophile is opening up the cyclopropyl ring, which could result in the new  $\text{CH}_2\text{N}$  and cause the mass to increase as shown in Figure 29.

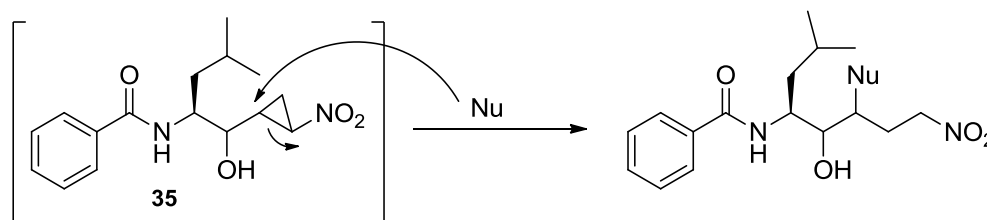


**Figure 29: Nucleophile attack on cyclopropyl ring**

## CHAPTER IV: CONCLUSIONS

Previous research in the lab had shown bioactivity for BACE inhibition in amides derived from the ester series, with the carbonyl of the amide adjacent to the cyclopropyl ring. The goal of this research was extend the series and to synthesize the counterpart “reverse” amides, with the nitrogen of the amide adjacent to the cyclopropyl ring. A key step in the synthesis was the incorporation of a nitro group beside the cyclopropyl ring to provide a handle for formation of the “reverse” amide. Nitrocyclopropanation is a method developed in the Dunlap laboratory using bromonitromethane to synthesize a cyclopropyl from a terminal amino-acid derived enone, providing a nitro group next to the ring as a precursor to an amine.

After synthesis of the cyclopropyl was complete, reduction of the nitro group was essential to form the “reverse” amide. Transfer hydrogenation using ammonium formate was found to reduce the nitro after removal of the Cbz-protecting group. Since the monoamine-nitro **32** was synthesized first, attempts were made to couple the amine to a known BACE side chain, N-dipropyl isophthalamide. Conditions already established in the Dunlap laboratory in the ester series, proved to be unsuccessful in the nitro series. An unexpected product is formed by what may be nucleophilic opening of the cyclopropyl ring, based on missing cyclopropyl signals in the  $^1\text{H}$  NMR and a new  $\text{CH}_2\text{N}$  signal in the  $^{13}\text{C}$  NMR. A similar result was seen even when coupling conditions were changed.

Further examination of the coupling conditions needs to be done in order to attach the BACE side chain to the core structure. The cyclopropyl ring is a key

conformational constraint in the products. Once the desired coupling product is synthesized, two steps remain reduction of the nitro group and coupling to various acids, to afford the reverse amides analogous to previously prepared amides.

## REFERENCES

1. Hebert, L. E.; Scherr, P. A.; Bienias, J. L.; Bennett, D. A.; and Evans, D. A. Alzheimer Disease in the US Population. *Arch. Neurol.* **2003**, *60*, 1119-1122.
2. Selkoe, Dennis J. Alzheimer's Disease: Genes, Proteins, and Therapy. *Physiol. Rev.* **2001**, *81*, 741-766.
3. US Dept. of Health and Human Services. National Plan to Address Alzheimer's Disease. **2011**, 1-63.
4. Alzheimer, Alois. A Characteristic Disease of the Cerebral Cortex. *Medizin.* **1907**, *44*, 146-148.
5. Glenner, G. G. and Wong, C.W. Alzheimer's disease: Initial Report of the Purification and Characterization of a Novel Cerebrovascular Amyloid Protein. *Biochem. Biophys. Res. Commun.* **1984**, *120*, 885-890.
6. Bouras, C.; Hof, P. R.; Giannakopoulos, P.; Michel, J. P.; and Morrison, J. H. Regional Distribution of Neurofibrillary Tangles and Senile Plaques in the Cerebral Cortex of Elderly Patients: A Quantitative Evaluation of a One-Year Autopsy Population from a Geriatric Hospital. *Cerebral Cortex* **1994**, *4*, 138-150.
7. Selkoe, Dennis J. The Molecular Pathology of Alzheimer's Disease. *Neuron.* **1991**, *6*, 487-498.
8. Hardy, J. A. and Higgins, G. A. Alzheimer's Disease: the Amyloid Cascade Hypothesis. *Science* **1992**, *256*, 184-185.
9. Haass, C. and Selkoe, D. J. Soluble Protein Oligomers in Neurodegeneration: Lessons from the Alzheimer's Amyloid  $\beta$ -Peptide. *Nature Reviews* **2007**, *8*, 101-112.
10. Grundke-Iqbal, I.; Iqbal, K.; Tung, Y.; Quinlan, M.; Wisniewski, H. M.; and Binder, L. I. Abnormal Phosphorylation of the Microtubule-Associated Protein  $\tau$  (Tau) in Alzheimer Cytoskeletal Pathology. *Proc. Natl. Acad. Sci. USA* **1986**, *83*, 4913-4917.
11. Kosik, K. S.; Joachim, C. L.; and Selkoe, D. J. Microtubule-Associated Protein  $\tau$  (Tau) is a Major Antigenic Component of Paired Helical Filaments in Alzheimer's Disease. *Proc. Natl. Acad. Sci. USA* **1986**, *83*, 4044-4048.
12. Nukina, N. and Ihara, Y. One of the Antigenic Determinants of Paired Helical Filaments is Related to  $\tau$  Protein. *J. Biochem.* **1986**, *99*, 1541-1544.
13. Iqbal, K. and Grundke-Iqbal, I. Mechanism of Alzheimer Neurofibrillary Degeneration and Formation of Tangles. *Mol. Psychiatry* **1997**, *2*, 178-80.
14. Delacourte, A. The Molecular Parameters of Tau Pathology. *Adv. Exp. Med. Biol.* **2001**, *487*, 5-19.
15. Hardy, J. and Selkoe, D. J. The Amyloid Hypothesis of Alzheimer's Disease: Progress and Problems on the Road to Therapeutics. *Science* **2002**, *297*, 353-356.
16. Korczyn, A. D. The Amyloid Cascade Hypothesis. *Alzheimer's & Dementia* **2008**, *4*, 176-178.

17. Kaufer-Nachum, D. Control and Peripheral Consequences of Cholinergic Imbalance in Alzheimer's Disease. In *Alzheimer Disease: From Molecular Biology to Therapy*; Becker, R. and Giacobini, E., Ed; Birkhauser: Boston, **1997**; pg 154.
18. Giacobini, E. Cholinesterase Inhibitors Do More than Inhibit Cholinesterase. In *Alzheimer Disease: From Molecular Biology to Therapy*; Becker, R. and Giacobini, E., Ed; Birkhauser: Boston, **1997**; pg 187.
19. Mehta, M.; Adem, A.; and Sabbagh, M. New Acetylcholinesterase Inhibitors for Alzheimer's Disease. *Int. J. Alzheimer's Disease* **2011**, *2012*, 1-8.
20. Moreira, P. I.; Zhu, X.; Nunomura, A.; Smith, M. A.; and Perry, G. Therapeutic Options in Alzheimer's Disease. *Expert Rev. Neurother.* **2006**, *6*, 897-910.
21. Terry, R. D.; Gonatas, N. K.; and Weiss, M. Ultrastructural Studies in Alzheimer's Presenile Dementia. *Am. J. Pathol.* **1964**, *44*, 269-297.
22. Glenner, G. G. and Wong, C. W. Alzheimer's Disease: Initial Report of the Purification and Characterization of a Novel Cerebrovascular Amyloid Protein. *Biochem. Biophys. Res. Comm.* **1984**, *120*, 885-890.
23. Masters, C. L.; Simms, G.; Weinman, N. A.; Multhaup, G.; McDonald, B. L.; and Beyreuther, K. Amyloid Plaque Core Protein in Alzheimer Disease and Down Syndrome. *Proc. Natl. Acad. Sci. USA.* **1985**, *82*, 4245-4249.
24. Haass, C. Take Five-BACE and the  $\gamma$ -secretase Quartet Conduct Alzheimer's Amyloid  $\beta$ -peptide Generation. *EMBO J.* **2004**, *22*, 483-488.
25. Esch, F. S.; Keim, P. S.; Beattie, E. C.; Blacher, R. W.; Culwell, A. R.; Oltersdorf, R.; McClure, D.; and Ward, P. J. Cleavage of Amyloid  $\beta$  Peptide During Constitutive Processing of Its Precursor. *Science* **1990**, *248*, 112-1124.
26. Sisodia, S. S.; Koo, E. H.; Beyreuther, K.; Unterbeck, A.; and Price, D. L. Evidence that  $\beta$ -Amyloid Protein in Alzheimer's Disease is Not Derived by Normal Processing. *Science* **1990**, *248*, 492-495.
27. Wisniewski, T.; Ghiso, J.; and Frangione, B. Peptides Homologous to the Amyloid Protein of Alzheimer's Disease Containing a Glutamine for Glutamic Acid Substitution Have Accelerated Amyloid Fibril Formation. *Biochem. Biophys. Res. Comm.* **1991**, *179*, 1247-1254.
28. Archer, H. A.; Edison, P.; Brooks, D. J.; Barnes, J.; Frost, C.; Yeatman, T.; Fox, N. C.; and Rossor, M. N. Amyloid Load and Cerebral Atrophy in Alzheimer's Disease: An  $^{11}\text{C}$ -PIB Positron Emission Tomography Study. *Ann. Neurol.* **2006**, *60*, 145-147.
29. Suzuki, N.; Cheung, T. T.; Cai, X.D.; Odaka, A.; Otvos, L. Jr.; Eckman, C.; Golde, T. E.; and Younkin, S. G. An Increased Percentage of Long Amyloid  $\beta$  Protein Secreted by Familial Amyloid  $\beta$  Protein Precursor ( $\beta\text{APP}_{717}$ ) Mutants. *Science* **1994**, *264*, 1336-1340.
30. Citron, M.; Oltersdorf, T.; Haass, C.; McConlogue, L.; Hung, A. Y.; Seuber, P.; Vigo-Pelfrey, C.; Lieberburg, I.; and Selkoe, D. J. Mutation of the  $\beta$ -amyloid Precursor Protein in Familial Alzheimer's Disease Increases  $\beta$ -protein Production. *Nature* **1992**, *360*, 672-674.
31. Hardy, J. Framing  $\beta$ -amyloid. *Nature Genetics* **1992**, *1*, 233-234.

32. Rapoport, M.; Dawson, H. N.; Binder, L. I.; Vitek, M. P.; and Ferreira, A. Tau is Essential to  $\beta$ -amyloid-induced Neurotoxicity. *Proc. Natl. Acad. Sci. USA* **2002**, *99*, 6364-6369.
33. Lewis, J.; Dickson, D. W.; Lin, W.L.; Chisholm, L.; Corral, A.; Jones, G.; Yen, S.H.; Sahara, N.; Skipper, L.; Yager, D.; Eckman, C.; Hardy, J.; Hutton, M.; and McGowan, E. Enhanced Neurofibrillary Degeneration in Transgenic Mice Expressing Mutant Tau and APP. *Science* **2001**, *293*, 1487-1491.
34. Hardy, J. Has the Amyloid Cascade Hypothesis for Alzheimer's Disease Been Proved? *Curr. Alzheimer Res.* **2006**, *3*, 71-73.
35. Hopkins, C. R. ACS Chemical Neuroscience Molecule Spotlight on ELND006: Another  $\gamma$ -Secretase Inhibitor Fails in the Clinic. *ACS Chem. Neurosci.* **2011**, *2*, 279-280.
36. Doody, R. S.; Raman, R.; Farlow, M.; Iwatsubo, T.; Vellas, B.; Joffe, S.; Keiburtz, K.; He, F.; Sun, X.; Thomas, R. G.; Aisen, P. S. Siemers, E.; Sethuraman, G.; and Mohs, R. A Phase 3 Trial of Semagacestat for Treatment of Alzheimer's Disease. *N. Engl. J. Med.* **2013**, *369*, 341-350.
37. Probst, G.; Aubele, D. L.; Bowers, S.; Dressen, D.; Garofalo, A. W.; Hom, R. K.; Konradi, A. W.; Marugg, J. L.; Mattson, M. N.; Neitzel, M. L.; Semko, C. M.; Sham, H. L.; Smith, J.; Sun, M.; Truong, A. P.; Ye, X. M.; Xu, Y.; Dappen, M. S.; Jagodzinski, J. J.; Keim, P. S.; Peterson, B.; Latimer, L. H.; Quincy, D.; Wu, J.; Goldbach, E.; Ness, D. K.; Quinn, K. P.; Sauer, J.M.; Wong, K.; Zhang, H.; Zmolek, W.; Brigham, E. F.; Kholodenko, D.; Hu, K.; Kwong, G. T.; Lee, M.; Liao, A.; Motter, R. H.; Sacayon, P.; Santiago, P.; Willits, C.; Bard, F.; Bova, M. P.; Hemphill, S. S.; Nguyen, L.; Ruslim, L.; Tanaka, K.; Tanaka, P.; Wallace, W.; Yednock, T. A.; and Basi, G. S. Discovery of (*R*)-4-Cyclopropyl-7,8-difluoro-5-(4-(trifluoromethyl)phenylsulfonyl)-4,5-dihydro-1*H*-pyrazolo[4,3-*c*]quinolone (ELND006) and (*R*)-4-Cyclopropyl-8-fluoro-5-(6-(trifluoromethyl)pyridine-3-ylsulfonyl)-4,5-dihydro-2*H*-pyrazolo[4,3-*c*]quinolone (ELND007): Metabolically Stable  $\gamma$ -Secretase Inhibitors that Selectively Inhibit the Production of Amyloid- $\beta$  over Notch. *J. Med. Chem.* **2013**, *56*, 5261-5274.
38. Sano, M. Tarenflurbil: Mechanisms and Myths. *Arch. Neurol.* **2010**, *67*, 750-752.
39. Sinha, S.; Anderson, J. P.; Barbour, R.; Basi, G. S.; Caccavello, R.; Davis, D.; Doan, M.; Dovey, H. F.; Frigon, N.; Hong, J.; Jacobson-Croak, K.; Jewett, N.; Keim, P. Knops, J.; Lieberburg, I.; Power, M.; Tan, H.; Tatsuno, G.; Tung, J.; Schenk, D.; Seubert, P.; Suomensaari, S. M.; Wang, S.; Walker, D.; Zhao, J.; McConlogue, L.; and John, V. Purification and Cloning of Amyloid Precursor Protein  $\beta$ -secretase from Human Brain. *Nature* **1999**, *402*, 537-540.
40. Yan, R.; Bienkowski, M. J.; Shuck, M. E.; Miao, H.; Tory, M. C.; Pauley, A. M.; Brashler, J. R.; Stratman, N. C.; Mathews, W. R.; Buhl, A. E.; Carter, D. B.; Tomasseli, A. G.; Parodi, L. A.; Heinrikson, R. L.; and Gurney, M. E. Membrane-anchored Aspartyl Protease with Alzheimer's Disease  $\beta$ -secretase Activity. *Nature* **1999**, *402*, 533-537.
41. Vassar, R.; Bennett, B. D.; Babu-Khan, S.; Kahn, S.; Mendiaz, E. A.; Denis, P.; Teplow, D. B.; Ross, S.; Amarante, P.; Loeloff, R.; Luo, Y.; Fisher, S.; Fuller, J.;

- Edenson, S.; Lile, J.; Jarosinski, M. A.; Biere, A. L.; Curran, E.; Burgess, T.; Louis, J.C.; Collins, F.; Treanor, J.; Rogers, G.; and Citron, M.  $\beta$ -Secretase Cleavage of Alzheimer's Amyloid Precursor Protein by the Transmembrane Aspartic Protease BACE. *Science* **1999**, *286*, 735-741.
42. Lin, X.; Koelsch, G.; Wu, S.; Downs, D.; Dashti, A.; and Tang, J. Human Aspartic Protease Memapsin 2 Cleaves the  $\beta$ -secretase Site of  $\beta$ -amyloid Precursor Protein. *Proc. Natl. Acad. Sci. USA* **2000**, *97*, 1456-1460.
43. Hussain, I.; Powell, D. J.; Howlett, D. R.; Chapman, G. A.; Gilmour, L.; Murdock, P. R.; Tew, D. G.; Meek, T. D.; Chapman, C.; Schneider, K.; Ratcliffe, S. J.; Tattersall, D.; Testa, T. T.; Southan, C.; Ryan, D. M.; Simmons, D. L.; Walsh, F. S.; Dingwall, C.; and Christie, G. ASP1 (BACE2) Cleaves the Amyloid Precursor Protein at the  $\beta$ -Secretase Site. *Mol. Cell. Neurosci.* **2000**, *16*, 609-619.
44. Venugopal, C.; Demos, C. M.; Rao, K. S. J.; Pappolla, M. A.; and Sambamurti, K. Beta-secretase: Structure, Function, and Evolution. *CNS Neurol Disord Drug Targets* **2008**, *7*, 278-294.
45. Solans, A.; Estivill, X.; and de La Luna, S. A New Aspartyl Protease on 21q22.3, BACE2, is Highly Similar to Alzheimer's Amyloid Precursor Protein  $\beta$ -secretase. *Cytogenet Cell Genet.* **2000**, *89*, 177-184.
46. Tomasselli, A. G.; Qahwash, I.; Emmons, T. L.; Lu, Y.; Leone, J. W.; Lull, J. M.; Fok, K. F.; Bannow, C. A.; Smith, C. W.; Bienkowski, M. J.; Henrikson, R. L.; and Yan, R. Employing a Superior BACE1 Cleavage Sequence to Probe Cellular APP Processing. *J. Neurochem.* **2003**, *84*, 1006-1017.
47. Hong, L.; Koelsch, G.; Lin, X.; Wu, S.; Terzyan, S.; Ghosh, A. K.; Zhang, X. C.; and Tang, J. Structure of the Protease Domain of Memapsin 2 ( $\beta$ -Secretase) Complexed with Inhibitor. *Science* **2000**, *290*, 150-153.
48. Mancini, F.; Simone, A. D.; and Andrisano, V. Beta-secretase as a Target for Alzheimer's Disease Drug Discovery: an Overview of *in vitro* Methods for Characterization of Inhibitors. *Anal. Bioanal. Chem.* **2011**, *400*, 1979-1996.
49. Yu, N.; Hayik, S. A.; Wang, B.; Liao, N.; Reynolds, C. H.; and Merz, K. M. Assigning the Protonation States of the Key Aspartates in  $\beta$ -Secretase Using OM/MM X-ray Structure Refinement. *J. Chem. Theory Comput.* **2006**, *2*, 1057-1069.
50. Shimizu, H. Tosaki, A.; Kaneko, K.; Hisano, T.; Sakurai, T.; and Nukina, N. Crystal Structure of an Active Form of BACE1, and Enzyme Responsible for Amyloid  $\beta$  Protein Production. *Mol. Cell Biol.* **2008**, *28*, 3663-3671.
51. Congreve, M.; Aharony, D.; Albert, J.; Callaghan, O.; Campbell, J.; Carr, R. A.; Chessari, G.; Cowan, S.; Edwards, P. D.; Frederickson, M.; McMenamin, R.; Murray, C. W.; Patel, S.; and Wallis, N. Application of Fragment Screening by X-ray Crystallography to the Discovery of Aminopyridines as Inhibitors of  $\beta$ -Secretase. *J. Med. Chem.* **2007**, *50*, 1124-1132.
52. Hong, L.; Turner, R. T.; Koelsch, G.; Shin, D.; Ghosh, A. K.; and Tang, J. Crystal Structure of Memapsin 2 ( $\beta$ -Secretase) in Complex with an Inhibitor OM00-3. *Biochemistry* **2002**, *41*, 10963-10967.

53. Gorfe, A. A.; and Caflisch, A. Functional Plasticity in the Substrate Binding Site of  $\beta$ -Secretase. *Structure* **2005**, *13*, 1487-1498.
54. Kamal, A.; Almenar-Queralt, A.; LeBlanc, J. F.; Roberts, E. A.; and Goldstein, L. S. B. Kinesin-mediated Axonal Transport of a Membrane Compartment Containing  $\beta$ -secretase and Presenilin-1 Requires APP. *Nature* **2001**, *414*, 643-648.
55. Hu, X.; Hicks, C. W.; He, W.; Wong, P.; Macklin, W. B.; Trapp, B. D.; and Yan, R. Bace1 Modulates Myelination in the Central and Peripheral Nervous System. *Nat. Neurosci.* **2006**, *9*, 1520-1525.
56. Rockenstein, E.; Mante, M.; Alford, M.; Adame, A.; Crews, L.; Hashimoto, M.; Esposito, L.; Mucke, L.; and Masliah, E. High  $\beta$ -Secretase Activity Elicits Neurodegeneration in Transgenic Mice Despite Reductions in Amyloid- $\beta$  Levels. *J. Biol. Chem.* **2005**, *280*, 32957-32967.
57. Johnston, J. A.; Liu, W. W.; Todd, S. A.; Coulson, D. T. R.; Murphy, S.; Irvine, G. B.; and Passmore, A. P. Expression and Activity of  $\beta$ -site Amyloid Precursor Protein Cleaving Enzyme in Alzheimer's Disease. *Biochem. Soc. Trans.* **2005**, *33*, 1096-1100.
58. Sastre, M.; Walter, J.; and Gentleman, S. M. Interactions Between APP Secretases and Inflammatory Mediators. *J. Neuroinflammation* **2008**, *5*, 1-11.
59. Cai, H.; Wang, Y.; McCarthy, D.; Wen, H.; Borchelt, D. R.; Price, D. L.; and Wong, P.C. BACE1 is the Major  $\beta$ -secretase for Generation of A $\beta$  Peptides by Neurons. *Nat. Neurosci.* **2001**, *4*, 233-234.
60. Luo, Y.; Bolon, B.; Kahn, S.; Bennett, B. D.; Babu-Khan, S.; Denis, P.; Fan, W.; Kha, H.; Zhang, J.; Gong, Y.; Martin, L.; Louis, J. C.; Yan, Q.; Richards, W. G.; Citron, M.; and Vassar, R. Mice Deficient in BACE1, the Alzheimer's  $\beta$ -secretase, Have Normal Phenotype and Abolished  $\beta$ -amyloid Generation. *Nat. Neurosci.* **2001**, *4*, 231-232.
61. Roberds, S. L.; Anderson, J.; Basi, G.; Bienkowski, M. J.; Branstetter, D. G.; Chen, K. S.; Freedman, S. B.; Frigon, N. L.; Games, D.; Hu, K.; Johnson-Wood, K.; Kappenman, K. E.; Kawabe, T. T.; Kola, I.; Kuehn, R.; Lee, M.; Liu, W.; Motter, R.; Nichols, N. R.; Power, M.; Robertson, D. W.; Schenk, D.; Schoor, M.; Shopp, G. M.; Shuck, M. E.; Sinha, S.; Svensson, K. A.; Tatsuno, G.; Tintrup, H.; Wijsman, J.; Wright, S.; and McConlogue, L. BACE Knockout Mice are Healthy Despite Lacking the Primary  $\beta$ -secretase Activity in Brain: Implications for Alzheimer's Disease Therapeutics. *Hum. Mol. Genet.* **2001**, *10*, 1317-1324.
62. McConlogue, L.; Buttini, M.; Anderson, J. P.; ... Partial Reduction of BACE1 has Dramatic Effects on Alzheimer Plaque and Synaptic Pathology in APP Transgenic Mice. *J. Biol. Chem.* **2007**, *282*, 26326-26334.
63. Ghosh, A. K.; Bilcer, G.; Harwood, C.; Kawahama, R.; Shin, D.; Hussain, K. A.; Hong, L.; Loy, J. A.; Nguyen, C.; Koelsch, G.; Ermolieff, J.; and Tang, J. Structure-Based Design: Potent Inhibitors of Human Brain Memapsin 2 ( $\beta$ -Secretase). *J. Med. Chem.* **2001**, *44*, 2865-2868.

64. Turner, R. T.; Koelsch, G.; Hong, L.; Castanheira, P.; Ghosh, A.; and Tang, J. Subsite Specificity of Memapsin 2 ( $\beta$ -secretase): Implications for Inhibitor Design. *Biochemistry* **2001**, *40*, 10001-10006.
65. Li, X.; Bo, H.; Zhang, X. C.; Hartsuck, J. A.; and Tang, J. Predicting Memapsin 2 (beta-secretase) Hydrolytic Activity. *Protein Sci.* **2010**, *19*, 2175-2185.
66. Kimura, T.; Hamada, Y.; Stochaj, M.; Ikari, H.; Nagamine, A.; Abdel-Rahman, H.; Igawa, N.; Hidaka, K.; Nguyen, J. T.; Saito, K.; Hayashi, Y.; and Kiso, Y. Design and Synthesis of Potent  $\beta$ -Secretase (BACE-1) Inhibitors with P<sub>1</sub>' Carboxylic Acid Bioisosteres. *Bioorg. Med. Chem. Lett.* **2006**, *16*, 2380-2386.
67. Hamada, Y.; Igawa, N.; Ikari, H.; Ziora, Z.; Nguyen, J. T.; Yamani, A.; Hidaka, K.; Kinura, T.; Saito, K.; Hayashi, Y.; Ebina, M.; Ishiura, S.; and Kiso, Y.  $\beta$ -Secretase Inhibitors: Modification at the P4 Position and Improvement of Inhibitory Activity in Cultured Cells. *Bioorg. Med. Chem. Lett.* **2006**, *16*, 4354-4359.
68. Lamar, J.; Hu, J.; Bueno, A. B.; Yang, H. C.; Guo, D.; Copp, J. D.; McGee, J.; Gitter, B.; Timm, D.; May, P.; McCarthy, J.; and Chen, S. H. *Bioorg. Med. Chem. Lett.* **2004**, *14*, 239-243.
69. Hom, R. K.; Gailunas, A. F.; Mamo, S.; Fang, L. Y.; Tung, J. S.; Walker, D. E.; Davis, D.; Thorsett, E. D.; Jewett, N. E.; Moon, J. B.; and John, V. Design and Synthesis of Hydroxyethylene-Based Peptidomimetic Inhibitors of Human  $\beta$ -Secretase. *J. Med. Chem.* **2004**, *47*, 158-164.
70. Wångsell, F.; Gustafsson, K.; Kvarnström, I.; Borkakoti, N.; Edlund, M.; Jansson, K.; Lindberg, J.; Hallberg, A.; Rosenquist, Å.; and Samuelsson, B. Synthesis of Potent BACE-1 Inhibitors Incorporating a Hydroxyethylene Isostere as Central Core. *Eur. J. Med. Chem.* **2010**, *45*, 870-882.
71. Björklund, C.; Oscarson, S.; Benkestock, K.; Borkakoti, N.; Jansson, K.; Lindberg, J.; Vrang, L.; Hallberg, A.; Rosenquist, Å.; and Samuelsson, B. Design and Synthesis of Potent and Selective BACE-1 Inhibitors. *J. Med. Chem.* **2010**, *53*, 1458-1464.
72. Meredith, J. A.; Björklund, C.; Adolfsson, H.; Jansson, K.; Hallberg, A.; Rosenquist, Å.; and Samuelsson, B. P2'-truncated BACE-1 Inhibitors With a Novel Hydroxyethylene-like Core. *Eur. J. Med. Chem.* **2010**, *45*, 542-554.
73. Ghosh, A. K.; Gemma, S.; and Tang, J.  $\beta$ -Secretase as a Therapeutic Target for Alzheimer's Disease. *Neurotherapeutics* **2008**, *5*, 399-408.
74. Stachel, S. J.; Coburn, C. A.; Steele, T. G.; Jones, K. G.; Loutzenhiser, E. F.; Grego, A. R.; Rajapakse, H. A.; Lai, M. T.; Crouthamel, M. C.; Xu, M.; Tugusheva, K.; Lineberger, J. E.; Pietrak, B. L.; Espeseth, A. S.; Shi, X. P.; Chen-Dodson, E.; Holloway, M. K.; Munshi, S.; Simon, A. J.; Kuo, L.; and Vacca, J. P. *J. Med. Chem.* **2004**, *47*, 6447-6450.
75. Maillard, M. C.; Hom, R. K.; Benson, T. E.; Moon, J. B.; Mamo, S.; Bienkowski, M.; Tomasselli, A. G.; Woods, D. D.; Prince, D. B.; Paddock, D. J.; Emmons, T. L.; Tucker, J. A.; Dappen, M. S.; Brogley, L.; Thorsett, E. D.; Jewett, N.; Sinha, S.; and John, V. Design, Synthesis, and Crystal Structure of Hydroxyethyl

- Secondary Amine-Based Peptidomimetic Inhibitors of Human  $\beta$ -Secretase. *J. Med. Chem.* **2007**, *50*, 776-781.
76. Freskos, J. N.; Fobian, Y. M.; Benson, T. E.; Bienkowski, M. J.; Brown, D. L.; Emmons, T. L.; Heintz, R.; Laborde, A.; McDonald, J. J.; Mischke, B. V.; Molyneaux, J. M.; Moon, J. B.; Mullins, P. B.; Prince, D. B.; Paddock, D. J.; Tomasselli, A. G.; and Winterrowd, G. Design of Potent Inhibitors of Human  $\beta$ -Secretase. Part I. *Bioorg. Med. Chem. Lett.* **2007**, *17*, 73-77.
77. Ghosh, A. K.; Kumaragurubaran, N.; Hong, L.; Kulkarni, S.; Xu, X.; Miller, H. B.; Reddy, D. S.; Weerasena, V.; Turner, R.; Chang, W.; Koelsch, G.; and Tang, J. Potent Memapsin 2 (beta-secretase) Inhibitors: Design, Synthesis, Protein-Ligand X-ray Structure, and *in vivo* Evaluation. *Bioorg. Med. Chem. Lett.* **2008**, *18*, 1031-1036.
78. Chang, W.; Huang, X.; Downs, D.; Cirrito, J.; Koelsch, G.; Holzman, D. M.; Ghosh, A. K.; and Tang, J.  $\beta$ -Secretase Inhibitor GRL-8234 Rescues Age-Related Cognitive Decline in APP Transgenic Mice. *FASEB J.* **2011**, *25*, 775-784.
79. Hussain, I.; Hawkins, J.; Harrison, D.; Hille, C.; Wayne, G.; Cutler, L.; Buck, T.; Walter, D.; Demont, E.; Howes, C.; Naylor, A.; Jeffrey, P.; Gonzalez, M. I.; Dingwall, C.; Michel, A.; Redshaw, S.; and Davis, J. B. *J. Neurochem.* **2007**, *100*, 802-809.
80. Iserloh, U.; Wu, Y.; Cumming, J. N.; Pan, J.; Wang, L. Y.; Stamford, A. W.; Kennedy, M. E.; Kuvelkar, R.; Chen, X.; Parker, E. M.; Strickland, C.; and Voigt, J. Potent Pyrrolidine- and Piperidine-Based BACE-1 Inhibitors. *Bioorg. Med. Chem. Lett.* **2008**, *18*, 414-417.
81. Cumming, J.; Babu, S.; Huang, Y.; Carrol, C.; Chen, X.; Favreau, L.; Greenlee, W.; Guo, T.; Kennedy, M.; Kuvelkar, R.; Le, T.; Li, G.; McHugh, N.; Orth, P.; Ozgur, L.; Parker, E.; Saionz, K.; Stamford, A.; Strickland, C.; Tadesse, D.; Voigt, J.; Zhang, L.; and Zhang, Q. Piperazine Sulfonamide BACE-1 Inhibitors: Design, Synthesis, and *in vivo* Characterization. *Bioorg. Med. Chem. Lett.* **2010**, *20*, 2837-2842.
82. Machauer, R.; Laumen, K.; Veenstra, S.; Rondeau, J. M.; Intelnot-Blomley, M.; Betschart, C.; Jaton, A. L.; Desrayaud, S.; Staufenbiel, M.; Rabe, S.; Paganetti, P.; and Neumann, U. *Bioorg. Med. Chem. Lett.* **2009**, *19*, 1366-1370.
83. Ghosh, A. K.; Devasamudram, T.; Hong, L.; DeZutter, C.; Xu, X.; Weerasena, V.; Koelsch, G.; Bilcer, G.; and Tang, J. *Bioorg. Med. Chem. Lett.* **2005**, *15*, 15-20.
84. Lindsley, S. R.; Moore, K. P.; Rajapakse, H. A.; Selnick, H. G.; Young, M. B.; Zhu, H.; Munshi, S.; Kuo, L.; McGaughey, G. B.; Colussi, D.; Crouthamel, M.; Lai, M.; Peitrak, B.; Price, E. A.; Sankaranarayanan, S.; Simon, A. J.; Seabrook, G. R.; Hazuda, D. J.; Pudvah, N. T.; Hochman, J. H.; Graham, S. L.; Vacca, J. P.; and Nantermet, P. G. Design, Synthesis, and SAR of Macrocyclic Tertiary Carbinamine BACE-1 Inhibitors. *Bioorg. Med. Chem. Lett.* **2007**, *17*, 4057-4061.
85. Lerchner, A.; Machauer, R.; Betschart, C.; Veenstra, S.; Rueeger, H.; McCarthy, C.; Intelnot-Blomley, M.; Jaton, A.; Rabe, S.; Desrayaud, S.; Enz, A.; Staufenbiel, M.; Paganetti, P.; Rondeau, J.; and Neumann, U. Macrocyclic

- BACE-1 Inhibitors Acutely Reduce A $\beta$  in Brain After Po Application. *Bioorg. Med. Chem. Lett.* **2010**, *20*, 603-607.
86. Stachel, S. J.; Coburn, C. A.; Sankaranarayanan, S.; Price, E. A.; Pietrak, B. L.; Huang, Q.; Lineberger, J.; Espeseth, A. S.; Jin, L.; Ellis, J.; Holloway, M. K.; Munshi, S.; Allison, T.; Hazuda, D.; Simon, A. J.; Graham, S. L.; and Vacca, J. P. Macrocyclic Inhibitors of  $\beta$ -Secretase: Functional Activity in an Animal Model. *J. Med. Chem.* **2006**, *49*, 6147-6150.
87. Ghosh, A. K.; Brindisi, M.; and Tang, J. Developing  $\beta$ -Secretase Inhibitors for Treatment of Alzheimer's Disease. *J. Neurochem.* **2012**, *120*, 71-83.
88. Stauffer, S. R.; Stanton, M. G.; Gregro, A. R.; Steinbeiser, M. A.; Shaffer, J. R.; Nantermet, R. G.; Barrow, J. C.; Rittle, K. E.; Collusi, D.; Espeseth, A. S.; Lai, M.; Pietrak, B. L.; Holloway, M. K.; McGaughey, G. B.; Munshi, S. K.; Hochman, J. H.; Simon, A. J.; Selnick, H. G.; Graham, S. L.; and Vacca, J. P. Discovery and SAR of Isonicotinamide BACE-1 Inhibitors that Bind Beta-secretase in a N-terminal 10s-loop Down Conformation. *Bioorg. Med. Chem. Lett.* **2007**, *17*, 1788-1792.
89. Stanton, M. G.; Stauffer, S. R.; Gregro, A. R.; Steinbeiser, M.; Nantermet, P.; Sankaranarayanan, S.; Price, E. A.; Wu, G.; Crouthamel, M.; Ellis, J.; Lai, M.; Espeseth, A. D.; Shi, X.; Jin, L.; Colussi, D.; Pietrak, B.; Huang, Q.; Xu, M.; Simon, A. J.; Graham, S. L.; Vacca, J. P. and Selnick, H. Discovery of Isonicotinamide Derived Beta-secretase Inhibitors: in vivo Reduction of Beta-amyloid. *J. Med. Chem.* **2007**, *50*, 3431-3433.
90. Zhu, H.; Young, M. B.; Nantermet, P. G.; Graham, S. L.; Colussi, D.; Lai, M.; Pietrak, B.; Price, E. A.; Sankaranarayanan, S.; Shi, X.; Tugusheva, K.; Halahan, M. A.; Michener, M. S.; Cook, J. J.; Simon, A.; Hazuda, D. J.; Vacca, J. P. and Rajapakse, H. A. Rapid P1 SAR of Brain Penetrant Tertiary Carbinamine Derived BACE Inhibitors. *Bioorg. Med. Chem. Lett.* **2010**, *20*, 1779-1782.
91. Cole, D. C.; Manas, E. S.; Stock, J. R.; Condon, J. S.; Jennings, L. D.; Aulabaugh, A.; Chopra, R.; Cowling, R.; Ellingboe, J. W.; Fan, K. Y.; Harrison, B. L.; Hu, Y.; Jacobsen, S.; Jin, G.; Lin, L.; Lovering, F. E.; Malamas, M. S.; Stahl, M. L.; Strand, J.; Sukhdeo, M. N.; Svenson, K.; Turner, M. J.; Wagner, E.; Wu, J.; Zhou, P.; and Bard, J. Acylguanidines as Small-Molecule  $\beta$ -Secretase Inhibitors. *J. Med. Chem.* **2006**, *49*, 6158-6161.
92. Fobare, W. F.; Solvibile, W. R.; Robichaud, A. J.; Malamas, M. S.; Manas, E.; Turner, J.; Hu, Y.; Wagner, E.; Chopra, R.; Cowling, R.; Jin, G.; and Bard, J. Thiophene Substituted Acylguanidines as BACE1 Inhibitors. *Bioorg. Med. Chem. Lett.* **2007**, *17*, 5353-5356.
93. Jennings, L. D.; Cole, D. C.; Stock, J. R.; Sukhdeo, M. N.; Ellingboe, J. W.; Cowling, R.; Jin, G.; Manas, E. S.; Fan, K. Y.; Malamas, M. S.; Harrison, B. L.; Jacobsen, S.; Chopra, R.; Lohse, P. A.; Moore, W. J.; O'Donnell, M.; Hu, Y.; Robichaud, A. J.; Turner, M. J.; Wagner, E.; and Bard, J. Acylguanidine Inhibitors of Beta-secretase: Optimization of the Pyrrole Ring Substituents Extending into the S1' Substrate Binding Pocket. *Bioorg. Med. Chem. Lett.* **2008**, *18*, 767-771.

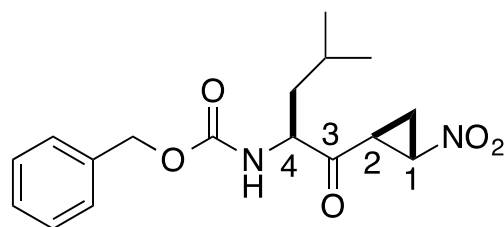
94. Cole, D. C.; Stock, J. R.; Chopra, R.; Cowling, R.; Ellingboe, J. W.; Fan, K. Y.; Harrison, B. L.; Hu, Y.; Jacobsen, S.; Jennings, L. D.; Jin, G.; Lohse, P. A.; Malamas, M. S.; Manas, E. S.; Moore, W. J.; O'Donnell, M.; Olland, A. M.; Robichaud, A. J.; Svenson, K.; Wu, J.; Wagner, E.; and Bard, J. Acylguanidine Inhibitors of Beta-secretase: Optimization of the Pyrrole Ring Substituents Extending into the S1 and S3 Substrate Binding Pockets. *Bioorg. Med. Chem. Lett.* **2008**, *18*, 1063-1066.
95. Baxter, E. W.; Conway, K. A.; Kennis, L.; Bischoff, F.; Mercken, M. H.; Winter, H. L.; Reynolds, C. H.; Tounge, B. A.; Luo, C.; Scott, M. K.; Huang, Y.; Braeken, M.; Pieters, S. M.; Berthelot, D. J.; Masure, S.; Bruinzeel, W. D.; Jordan, A. D.; Parker, M. H.; Boyd, R. E.; Qu, J. Alexander, R. S.; Brenneman, D. E.; and Reitz, A. B. 2-Amino-3,4-dihydroquinazolines as Inhibitors of BACE-1 (beta-site APP cleaving enzyme): Use of Structure Based Design to Convert a Micromolar Hit Into a Nanomolar Lead. *J. Med. Chem.* **2007**, *50*, 4261-4264.
96. <http://www.alzforum.org/new/detail.asp?id=1790>
97. Hey, J. A.; Koelsch, G.; Bilcer, G.; Jacobs, A.; Tolar, M.; Tang, J.; Ghosh, A. K.; and Hsu, H. H. Single Dose Administration of the  $\beta$ -Secretase Inhibitor CTS21166 (ASP1702) Reduces Plasma A $\beta$ 40 in Human Subjects. *International Conference on Alzheimer's Disease (ICAD)*, Chicago, IL, **2008**.
98. Koelsch, G.; Tang, J.; Ghosh, A. K.; Bilcer, G.; Hey, J. A.; and Windisch, M. BACE1 Inhibitor CTS21166 (ASP1702) Penetrates Brain and Reduces A $\beta$  Pathology in a Transgenic Mouse Model of Advanced AD. *International Conference on Alzheimer's Disease (ICAD)*, Chicago, IL, **2008**.
99. Shitaka, Y.; Yarimizu, J.; Nagakura, A.; Mitani, Y.; Takami, S.; Miyake, A.; Hamakawa, N.; Hey, J. A.; Koelsch, G.; Bilcer, G.; and Matsuoka, N. Oral Administration of the BACE1 Inhibitor CTS21166 (ASP1702) Improves Cognition and Reduces Brain A $\beta$  in Tg2576 Transgenic Mice. *International Conference on Alzheimer's Disease (ICAD)*, Chicago, IL, **2008**.
100. Luo, X.; and Yan, R. Inhibition of BACE1 for Therapeutic Use in Alzheimer's Disease. *Int. J. Clin. Exp. Pathol.* **2010**, *3*, 618-628.
101. Vagner, J.; Qu, H.; and Hruby, V. J. Peptidomimetics, A Synthetic Tool of Drug Discover. *Curr. Op. Chem. Bio.* **2008**, *12*, 292-296.
102. Liskamp, R. M. J.; Rijkers, D. T. S.; Kruijtzter, J. A. W.; and Kemmink, J. Peptides and Proteins as a Continuing Exciting Source of Inspiration for Peptidomimetics. *ChemBioChem* **2011**, *12*, 1626-1653.
103. Jamieson, A. G.; Boutard, N.; Sabatino, D.; and Lubell, W. D. Peptide Scanning for Studying Structure-Activity Relationships in Drug Discovery. *Chem. Bio. Drug Des.* **2013**, *81*, 148-165.
104. Hruby, V. J.; and Cai, M. Design of Peptide and Peptidomimetic Ligands with Novel Pharmacological Activity Profiles. *Annu. Rev. Pharmacol. Toxicol.* **2013**, *53*, 557-580.
105. Hill, D. J.; Mio, M. J.; Prince, R. B.; Hughes, T. S.; and Moore, J. S. A Field Guide to Foldamers. *Chem. Rev.* **2001**, *101*, 3893-4011.

106. Veber, D. F.; Johnson, S. R.; Cheng, H. Y.; Smith, B. R.; Ward, K. W.; and Kopple, K. D. Molecular Properties that Influence the Oral Bioavailability of Drug Candidates. *J. Med. Chem.* **2002**, *45*, 2615-2623.
107. Romero, A. G.; Darlington, W. H.; Piercey, M. F.; and Lahti, R. A. *Bioorg. Med. Chem. Lett.* **1992**, *2*, 1703-1706.
108. Diana, G. D.; Rudewicz, P.; Pevear, D. C.; Nitz, T. J.; Aldous, S. C.; Aldous, D. J.; Robinson, D. T.; Draper, T.; Dutko, F. J.; Aldi, C.; Gendron, G.; Oglesby, R. C.; Volkots, D. L.; Reuman, M.; Bailey, T. R.; Czerniak, R.; Block, T.; Roland, R.; and Oppermann, J. *J. Med. Chem.* **1995**, *38*, 1355-1371.
109. Martin, S. F.; Dorsey, G. O.; Gane, T.; Hilier, M. C.; Kessler, H.; Baur, M.; Mathä, B.; Erickson, J. W.; Bhat, T. N.; Munshi, S.; Gulnik, S. V.; and Topol, I. A. Cyclopropane-Derived Peptidomimetics. Design, Synthesis, Evaluation, and Structure of Novel HIV-1 Protease Inhibitors. *J. Med. Chem.* **1998**, *41*, 1581-1597.
110. Hillier, M. C.; Davidson, J. P.; and Martin, S. F. Cyclopropane-Derived Peptidomimetics. Design, Synthesis, and Evaluation of Novel Ras Farnesyltransferase Inhibitors. *J. Org. Chem.* **2001**, *66*, 1657-1671.
111. Reichelt, A.; and Martin, S. F. Synthesis and Properties of Cyclopropane-Derived Peptidomimetics. *Acc. Chem. Res.* **2006**, *39*, 433-442.
112. Milanole, G.; Couve-Bonnaire, S.; Bonfanti, J-F. Jubault, P.; and Pannecoucke, X. Synthesis of Fluorinated Cyclopropyl Amino Acid Analogues: Toward the Synthesis of Original Fluorinated Peptidomimetics. *J. Org. Chem.* **2013**, *78*, 212-223.
113. Martin, S. F.; Austin, R. E.; Oalman, C. J.; Baker, W. R.; Condon, S. L.; deLara, E.; Rosenberg, S. H.; Spina, K. P.; Stein, H. H.; Cohen, J.; and Kleinert, H. D. 1,2,3-Trisubstituted Cyclopropanes as Conformationally Restricted Peptide Isosteres: Application to the Design and Synthesis of Novel Renin Inhibitors. *J. Med. Chem.* **1992**, *35*, 1710-1721.
114. Williams, D. H.; Stephens, E.; O'Brien, D. P.; and Zhou, M. Understanding Noncovalent Interactions: Ligand Binding Energy and Catalytic Efficiency from Ligand-Induced Reductions within Receptors and Enzymes. *Angew. Chem., Int. Ed.* **2004**, *43*, 6596-6616.
115. Kempf, D. J.; Codacovi, L.; Wang, X. C.; Kohlbrenner, W. R.; Wideburg, N. E.; Saldivar, A.; Vasavanonda, S.; Marsh, K. D.; Bryant, P. Sham, H. L.; Green, B. E.; Betebenner, D. A.; Erickson, J.; and Norbeck, D. W. Symmetry-Based Inhibitors of HIV Protease. Structure-Activity Studies of Acylated 2,4-Diamino-1,5-diphenyl-3-hydroxypentane and 2,5-Diamino-1,6-diphenylhexane-3,4-diol. *J. Med. Chem.* **1993**, *36*, 320-330.
116. Wipf, P.; and Xiao, J. Convergent Approach to (E)-Alkene and Cyclopropane Peptide Isosteres. *Org. Lett.* **2005**, *7*, 103-106.
117. Wipf, P.; and Stephenson, C. R. J. Three-Component Synthesis of  $\alpha,\beta$ -Cyclopropyl- $\gamma$ -Amino Acids. *Org. Lett.* **2005**, *7*, 1137-1140.
118. Wipf, P.; Werner, S.; Woo, G. H. C.; Stephenson, C. R. J.; Walczak, M. A. A.; Coleman, C. M.; and Twining, L. A. Application of Divergent Multi-Component

- Reactions in the Synthesis of a Library of Peptidomimetics Based on  $\gamma$ -Amino- $\alpha,\beta$ -cyclopropyl Acids. *Tetrahedron* **2005**, *61*, 11488-11500.
119. Dunlap, N.; Lankford, K. R.; Pathiranage, A. L.; Taylor, J.; Reddy, N.; Gouger, D.; Singer, P.; Griffin, K.; and Reibenspies, J. Three-Step Synthesis of Cyclopropyl Peptidomimetics. *Org. Lett.* **2011**, *13*, 4879-4881.
  120. Dunlap, N. K.; Basham, J.; Wright, M.; Smith, K.; Chapa, O.; Huang, J.; Shelton, W.; and Yatsky, Y. Synthesis of Nitrocyclopropyl Peptidomimetics. *Tetrahedron Lett.* **2013**, *54*, 6596-6598.
  121. Braish, T. F.; Castaldi, M.; Chan, S.; Fox, D. E.; Keltonic, T.; McGarry, J.; Hawkins, J. M.; Norris, T.; Rose, P. R.; Sieser, J. E.; Sitter, B. J.; and Watson, H. Construction of the (1-,5-,6-)6-Amino-3-azabicyclo[3.1.0]hexane Ring System. *Synlett.* **1996**, 1100-1102.
  122. Ballini, R.; Fiorini, D.; and Palmieri, A. A General Procedure for the One-pot Preparation of Polyfunctionalized Nitrocyclopropanes. *Synlett.* **2003**, *11*, 1704-1706.
  123. Wascholowski, V.; Hansen, H. N.; Longbottom, D. A.; and Ley, S. V. A General Organocatalytic Enantioselective Nitrocyclopropanation Reaction. *Synthesis* **2008**, 1269-1275.
  124. CECAD Cologne. Principal Investigators: Dr. Markus Schubert. <http://www.cecad-cologne.de/index.php?id=106> (accessed 2 October 2013).
  125. Umbreen, S.; Brockhaus, M.; Ehrenberg, H.; and Schmidt, B.; Norstatines from Aldehydes by Sequential Organocatalytic  $\alpha$ -Amination and Passerini Reaction. *European Journal of Organic Chemistry* **2006**, *20*, 4585-4595.
  126. Barrett, A. G. M.; and Spilling, C. D. Transfer Hydrogenation: A Stereospecific Method for the Conversion of Nitro Alkanes into Amines. *Tetrahedron Lett.* **1988**, *29*, 5733-5734.
  127. Ram, S.; and Ehrenkauf, R. E. A General Procedure for Mild and Rapid Reduction of Aliphatic and Aromatic Nitro Compounds Using Ammonium Formate as a Catalytic Hydrogen Transfer Agent. *Tetrahedron Lett.* **1984**, *25*, 3415-3418.
  128. Ram, S.; and Ehrenkauf, R. E. A Facile Synthesis of  $\alpha$ -Amino Esters via Reduction of  $\alpha$ -Nitro Esters Using Ammonium Formate as a Catalytic Hydrogen Transfer Agent. *Communications* **1986**, *1*, 133-135.

**APPENDIX: NMR SPECTROSCOPY DATA**

**Benzyl ((*S*)-4-methyl-1-((1*S*,2*S*)-2-nitrocyclopropyl)-1-oxopentan-2-yl)carbamate  
(*syn*-30)**



-NMR

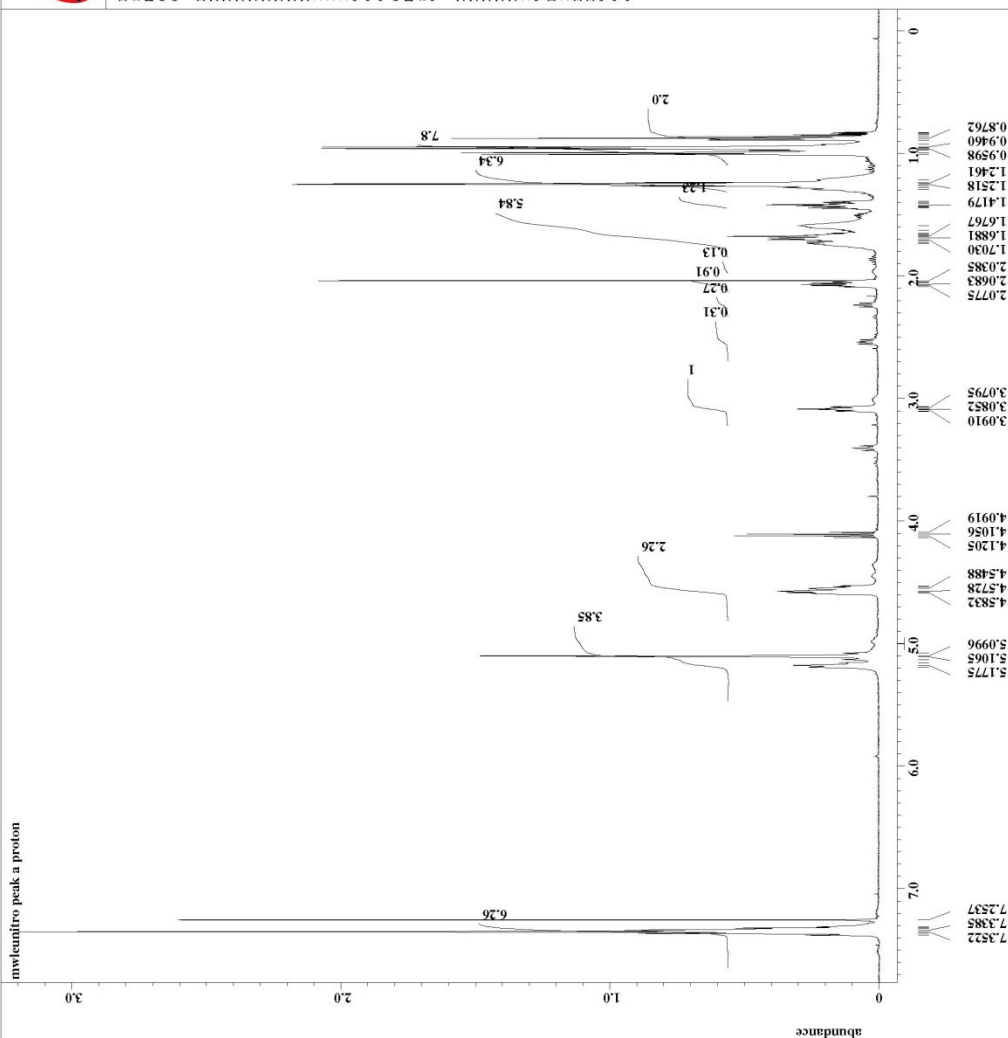
-<sup>1</sup>H



Filename = 09281euniro.peak a P  
Sample\_id = 09281euniro.peak a P  
Machine = mcau500sp  
Creation\_time = 28-SEP-2012 09:49:49  
Comment = mwLeuniro.peak a Pro

Field strength = 11.7473579[T] (500[MH]  
X\_acq\_duration = 1.74587904[s]  
X\_domain = LH  
X\_freq = 500.15991521[MHz]  
X\_offset = 0.0[ppm]  
X\_points = 16384  
X\_prescans = 1  
X\_resolution = 0.57277737[Hz]  
X\_sweep = 9.38438438[kHz]  
X\_domain = LH  
Irr\_freq = 500.15991521[MHz]  
Irr\_offset = 5.0[ppm]  
Tri\_domain = LH  
Tri\_freq = 500.15991521[MHz]  
Tri\_offset = 0.0[ppm]  
Clipped = FALSE  
Mod\_return = 1  
Scans = 1  
Total\_scans = 16

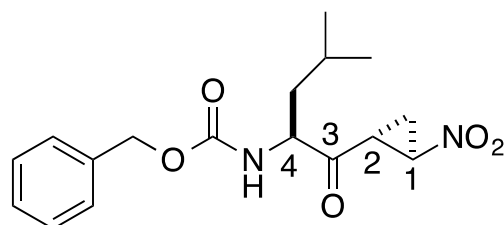
X\_90\_width = 13.802[us]  
X\_acq\_time = 1.74587904[s]  
X\_angle = 45[deg]  
X\_atn = 3[db]  
X\_pulse = 6.90[us]  
X\_mode = Off  
Tri\_mode = Off  
Dante\_preat = FALSE  
Initial\_wait = 1[s]  
Relaxation\_delay = 4[s]  
Repetition\_time = 5.74587904[s]  
Temp\_atate = TEMP OFF  
Temp\_set = 25[degC]  
Temp\_get = 21.7[degC]



X : parts per Million : 1H

**Benzyl ((*S*)-4-methyl-1-((1*R*,2*R*)-2-nitrocyclopropyl)-1-oxopentan-2-yl)carbamate**

**(*anti*-30)**



-NMR

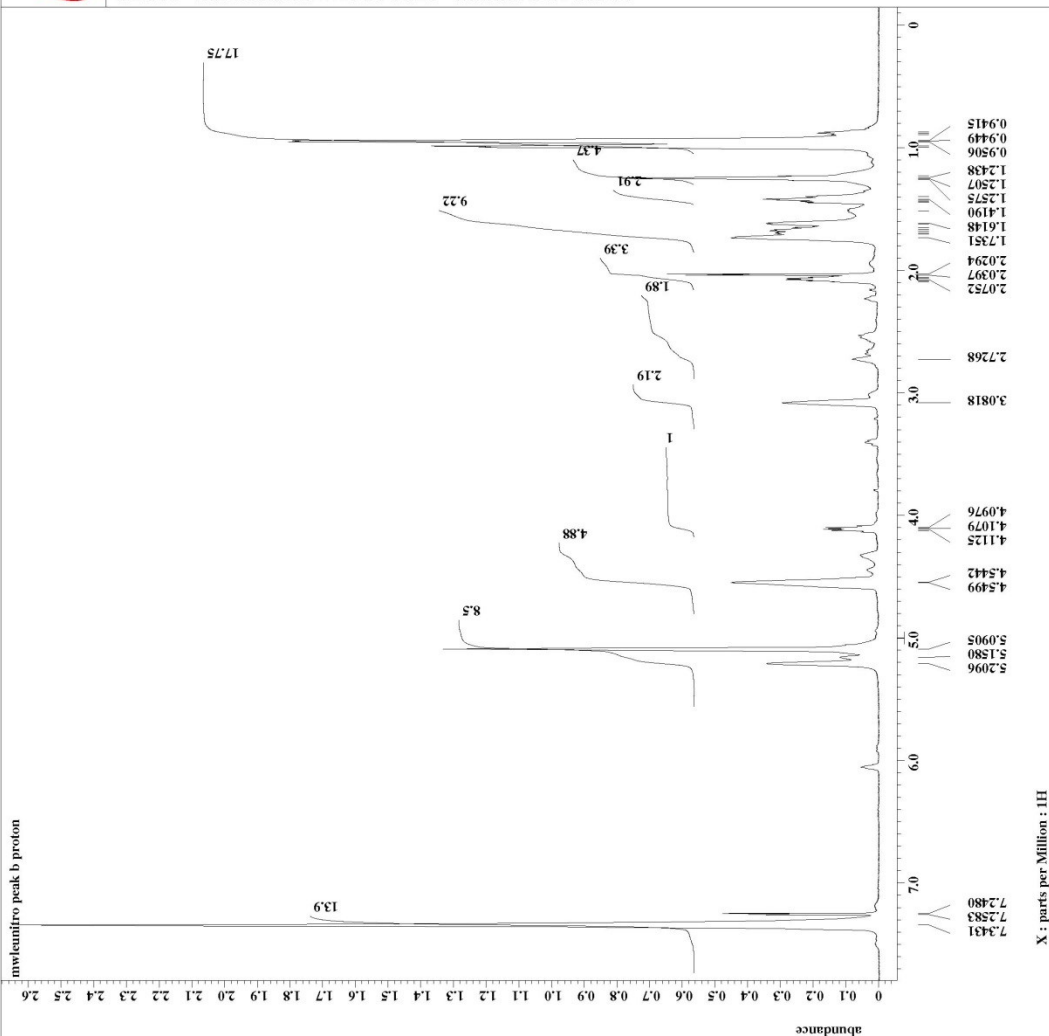
-<sup>1</sup>H



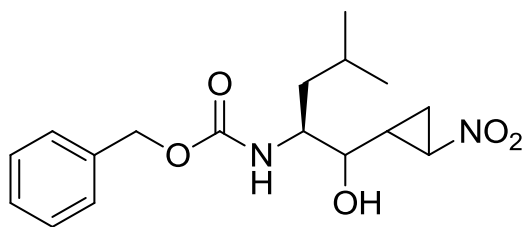
Filename = 09281euniro.peak b p  
Sample\_id = 09281euniro.peak b p  
Machine = mca500sp  
Creation\_time = 28-SEP-2012 10:23:47  
Comment = mwLeuniro.peak b Pro

Field strength = 11.7473579[T] (500[MH  
X\_acq\_duration = 1.74587904[s]  
X\_domain = 1H  
X\_freq = 500.15991521[MHz]  
X\_offset = 0.0[ppm]  
X\_points = 16384  
X\_prescans = 1  
X\_resolution = 0.57277737[Hz]  
X\_sweep = 9.38438438[kHz]  
X\_domain = 1H  
Irr\_freq = 500.15991521[MHz]  
Irr\_offset = 5.0[ppm]  
Tri\_domain = 1H  
Tri\_freq = 500.15991521[MHz]  
Tri\_offset = 0.0[ppm]  
Clipped = FALSE  
Mod\_return = 1  
Scans = 16  
Total\_scans = 16

X\_90\_width = 13.802[us]  
X\_acq\_time = 1.74587904[s]  
X\_angle = 45[deg]  
X\_atn = 3[db]  
X\_pulse = 6.90[us]  
Tri\_mode = Off  
Tri\_mode = Off  
Dante\_preat = FALSE  
Initial\_wait = 1[s]  
Relaxation\_delay = 4[s]  
Repetition\_time = 5.0487904[s]  
Temp\_atate = TEMP\_OFF  
Temp\_set = 25[dc]  
Temp\_get = 21.8[dc]



X : parts per Million : 1H

**Benzyl ((2*S*)-1-(2-nitrocyclopropyl)-1-hydroxy-4-methylpentan-2-yl)carbamate 31**

-NMR

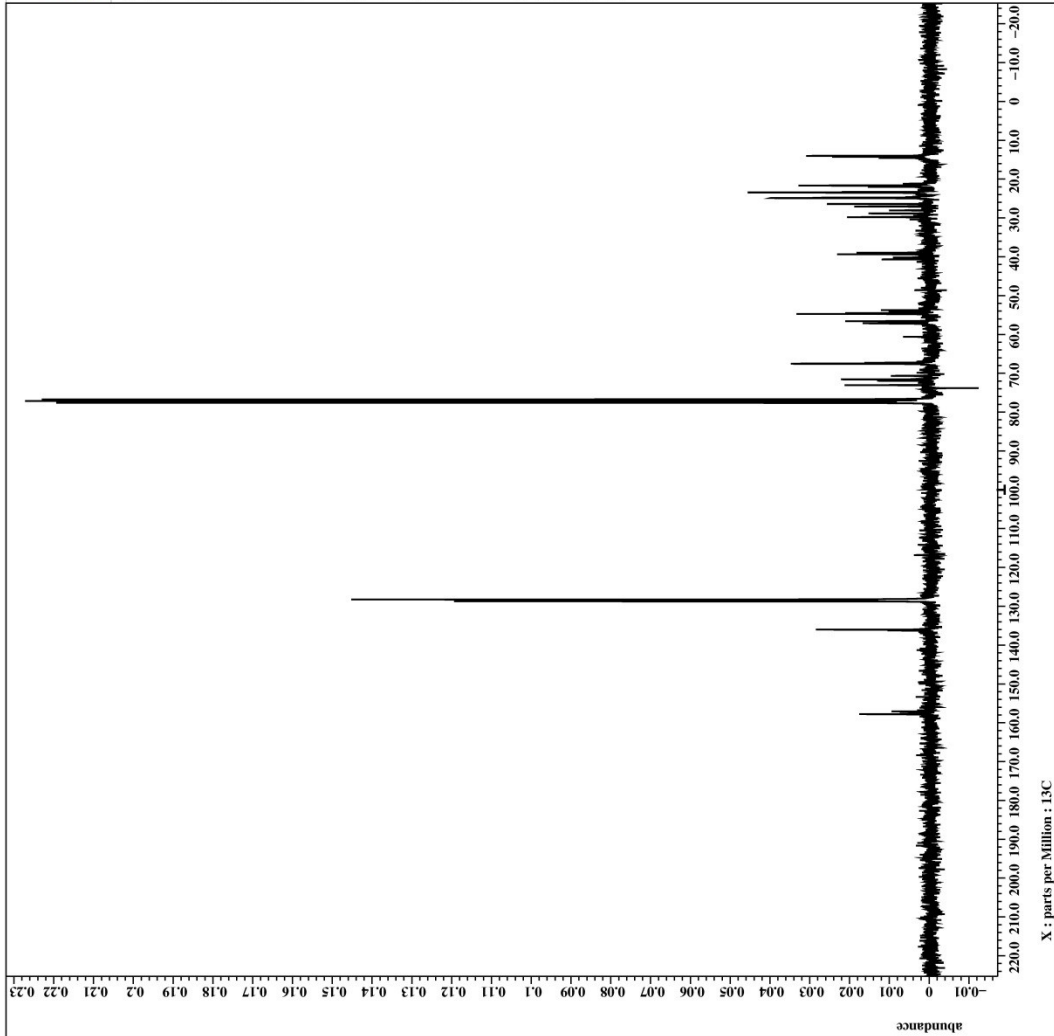
-<sup>1</sup>H

-<sup>13</sup>C

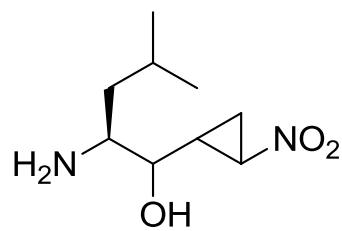




Filename = KS49\_CARBON-4\_jdf  
Sample\_id = KS49  
Machine = mtsu300sp  
Creation\_time = 3-APR-2013 13:29:26  
Field\_strength = 7.0586013(T) (300 [MHz]  
X\_acq\_duration = 1.38412032[s]  
X\_domain = 13C  
X\_freq = 75.56823426 [MHz]  
X\_offset = 20 [ppm]  
X\_offset2 = 27.68  
X\_prescans = 4  
X\_resolution = 0.72248054 [Hz]  
X\_sweep = 23.67424242 [kHz]  
Irr\_domain = IR  
Irr\_freq = 40.52965592 [MHz]  
Irr\_offset = 5 [ppm]  
Clipped = TRUE  
Mod\_return = 1  
Scans = 541  
Total\_scans = 541  
X\_90\_width = 12.643 [us]  
X\_acq\_time = 1.38412032 [s]  
X\_angle = 30 [deg]  
X\_atn = 9 [dB]  
X\_pulse = 9 [24.433333 [us]  
Irr\_atn\_dec = 24.6 [dB]  
Irr\_atn\_noe = WALTZ  
Decoupling = TRUE  
Puls1\_wait = TRUE  
Noe\_time = 2 [s]  
Relaxation\_delay = 2 [s]  
Repetition\_time = 3.38412032 [s]  
Temp\_set = 25 [degC]  
Temp\_get = 19.9 [degC]



X : parts per Million : 13C

**(2*S*)-2-amino-4-methyl-1-(2-nitrocyclopropyl)pentan-1-ol (32)**

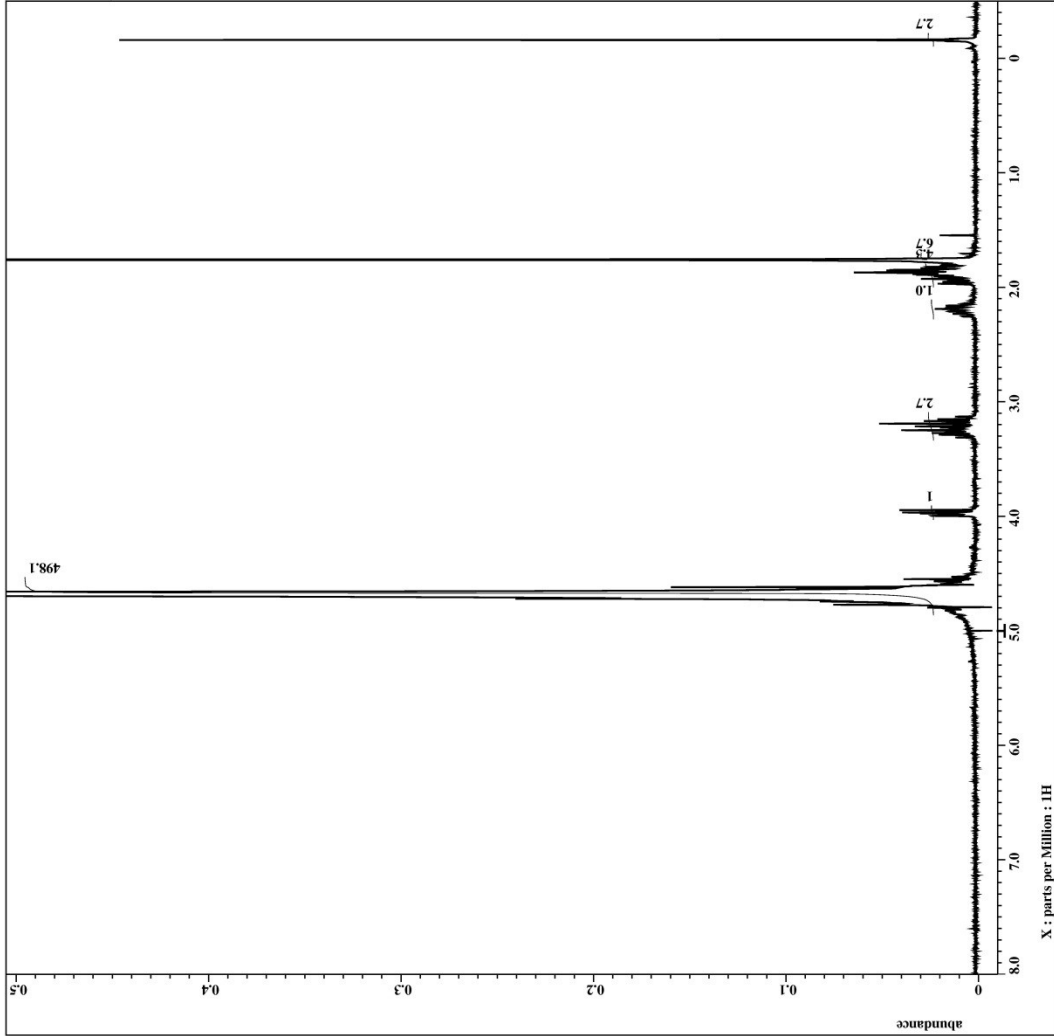
-NMR

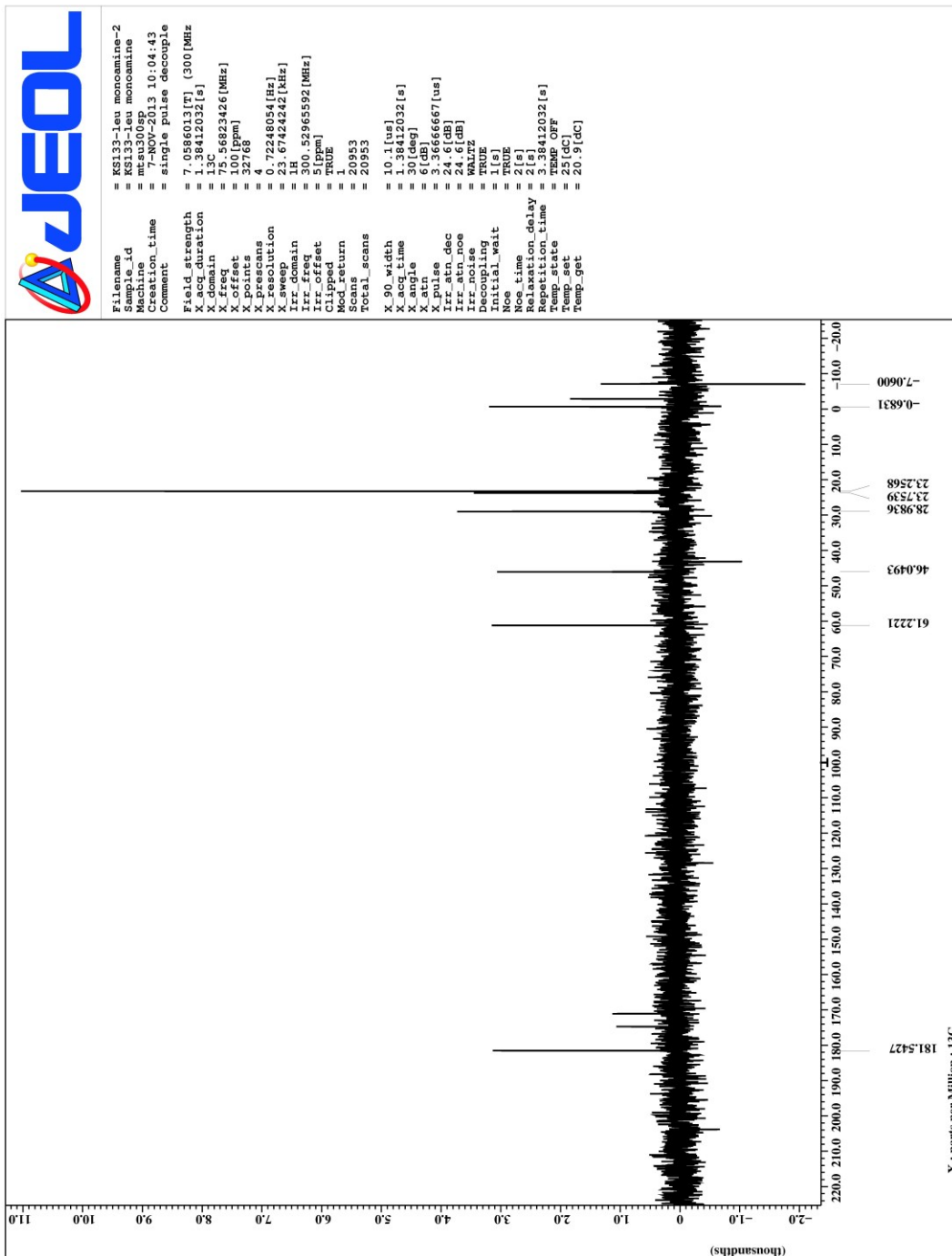
-<sup>1</sup>H

-<sup>13</sup>C



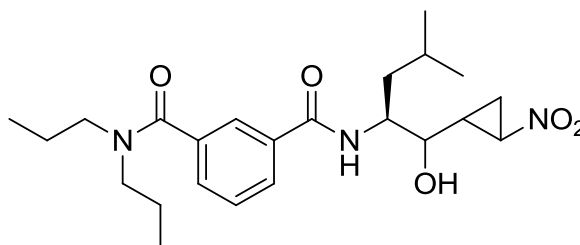
Filename = KSI133-leu\_monocamine\_P  
Sample\_id = KSI133-leu\_monocamine  
Machine = mtsu300sp  
Creation\_time = 6-NOV-2013 14:08:32  
Comment = from ammonium formate  
Field\_strength = 7.0586013[T] (300[MHz]  
X\_acq\_duration = 2.90717696[s]  
X\_domain = 1H  
X\_freq = 300.52965592[MHz]  
X\_gain = 16384  
X\_points = 1  
X\_prescans = 1  
X\_resolution = 0.34397631[Hz]  
X\_sweep = 5.63570784[kHz]  
X\_domain = 1H  
Irr\_freq = 300.52965592[MHz]  
Irr\_offset = 5[ppm]  
Tri\_domain = 1H  
Tri\_freq = 300.52965592[MHz]  
Tri\_offset = 5[ppm]  
Clipped = FALSE  
Mod\_return = 1  
Scans = 64  
Total\_scans = 64  
X\_90\_width = 12.7[us]  
X\_acq\_time = 2.90717696[s]  
X\_angle = 45[deg]  
X\_atn = 3[db]  
X\_pulse = 6.25[us]  
X\_mode = Off  
Tri\_mode = Off  
Dante\_preat = FALSE  
Initial\_wait = 1[s]  
Relaxation\_delay = 4[s]  
Repetition\_time = 2.90717696[s]  
Temp\_set = 25[degC]  
Temp\_get = 20.7[degC]





X : parts per Million : 13C

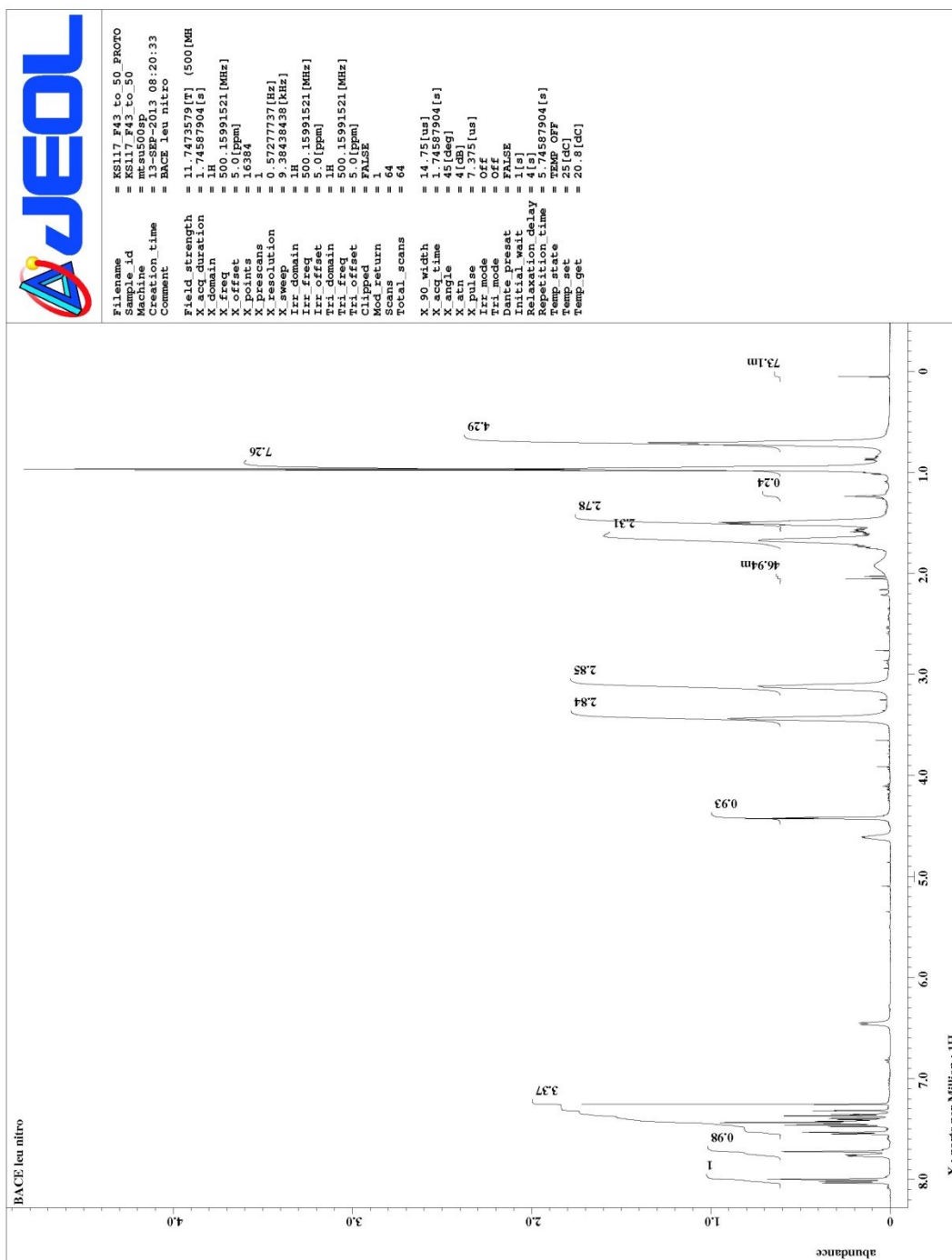
**N1-((2S)-1-hydroxy-4-methyl-1-(2-nitrocyclopropyl)pentan-2-yl)-N3,N3-dipropylisophthalamide (34)**

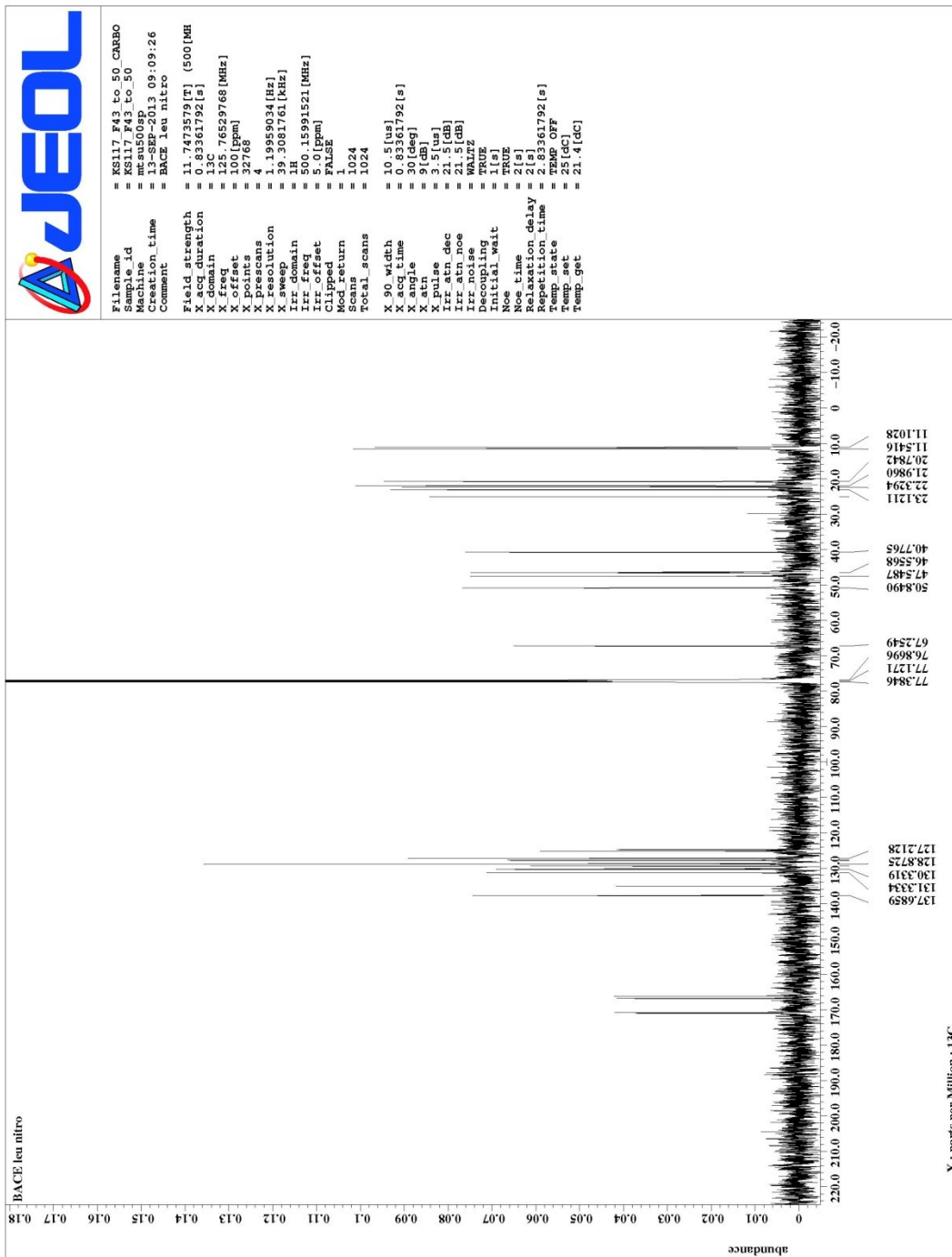


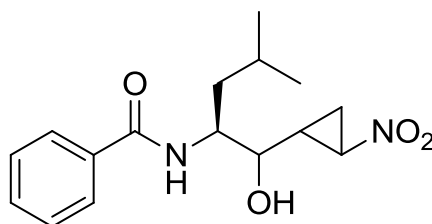
-NMR

-<sup>1</sup>H

-<sup>13</sup>C





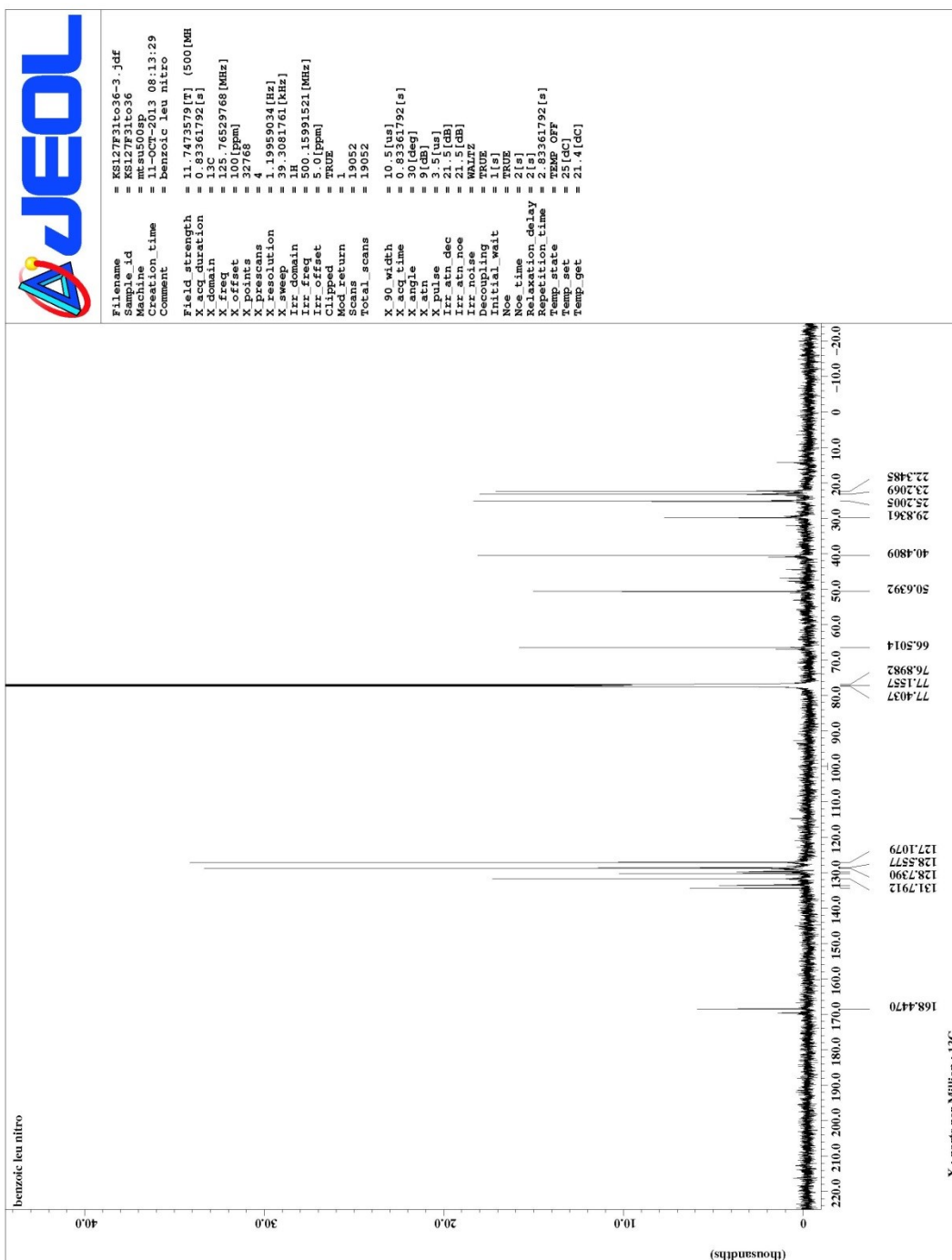
**N-((2S)-1-hydroxy-4-methyl-1-(2-nitrocyclopropyl)pentan-2-yl)benzamide (35)**

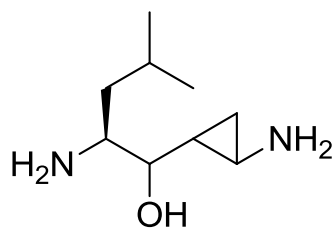
-NMR

-<sup>1</sup>H

-<sup>13</sup>C

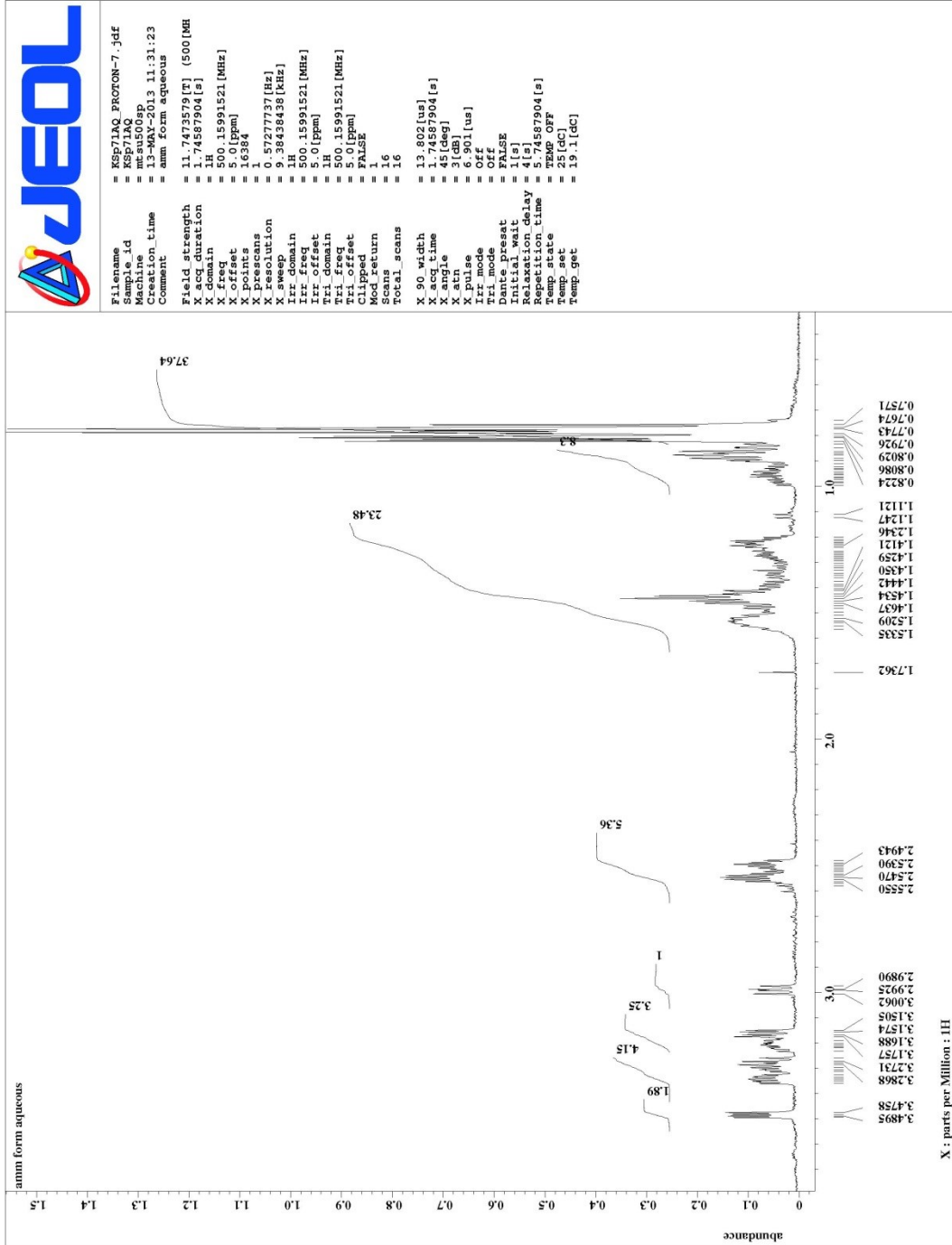




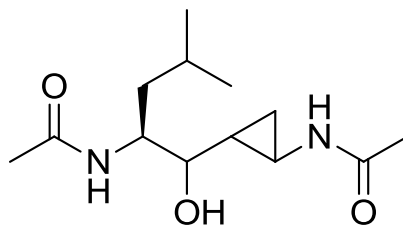
**(2*S*)-2-amino-1-(2-aminocyclopropyl)-4-methylpentan-1-ol (36)**

-NMR

-<sup>1</sup>H



*N*-(2-((2*S*)-2-acetamido-1-hydroxy-4-methylpentyl)cyclopropyl)acetamide (37)



-NMR

-<sup>1</sup>H

